

**Phase transitions and order in two-dimensional generalized nonlinear  $\sigma$  models**Tirthankar Banerjee,<sup>1,\*</sup> Niladri Sarkar,<sup>1,2,†</sup> and Abhik Basu<sup>1,‡</sup><sup>1</sup>*Condensed Matter Physics Division, Saha Institute of Nuclear Physics, Calcutta 700064, India*<sup>2</sup>*Max-Planck Institut für Physik Komplexer Systeme, Nöthnitzer Str. 38, Dresden, D-01187 Germany*

(Received 10 August 2015; published 18 December 2015)

We study phase transitions and the nature of order in a class of classical generalized  $O(N)$  nonlinear  $\sigma$  models (NLS) constructed by minimally coupling pure NLS with additional degrees of freedom in the form of (i) Ising ferromagnetic spins, (ii) an advective Stokesian velocity, and (iii) multiplicative noises. In examples (i) and (ii), and also (iii) with the associated multiplicative noise being not sufficiently long-ranged, we show that the models may display a class of unusual phase transitions between *stiff* and *soft phases*, where the effective spin stiffness respectively diverges and vanishes in the long wavelength limit at two dimensions (2D), unlike in pure NLS. In the stiff phase, in the thermodynamic limit the variance of the transverse spin (or, the Goldstone mode) fluctuations are found to scale with the system size  $L$  in 2D as  $\ln \ln L$  with a model-dependent amplitude, which is markedly weaker than the well-known  $\ln L$  dependence of the variance of the broken symmetry modes in models that display quasi-long-range order in 2D. Equivalently, for  $N = 2$  at 2D the equal-time spin-spin correlations decay in powers of inverse logarithm of the spatial separation with model-dependent exponents. These transitions are controlled by the model parameters those couple the  $O(N)$  spins with the additional variables. In the presence of long-range noises in example (iii), true long-range order may set in 2D, depending upon the specific details of the underlying dynamics. Our results should be useful in understanding phase transitions in equilibrium and nonequilibrium low-dimensional systems with continuous symmetries in general.

DOI: [10.1103/PhysRevE.92.062133](https://doi.org/10.1103/PhysRevE.92.062133)

PACS number(s): 64.60.De, 64.60.Ht, 64.60.ae

**I. INTRODUCTION**

Understanding phase transitions and order in low-dimensional systems has remained a topic of considerable theoretical interests. For two-dimensional (2D) systems in equilibrium with continuous symmetries and short-range interactions, there is no phase transition to a low-temperature ( $T$ ) broken symmetry phase with long-range order (LRO) at any  $T \neq 0$ . This is a consequence of the well-known Mermin-Wagner theorem (MWT) [1]. As a result in the thermodynamic limit (TL), there is no statistically flat phase of a fluid membrane or a 2D crystal in thermal equilibrium. In contrast, LRO in 2D equilibrium systems can exist at a finite  $T$  if there are effective long-range interactions present in the system which can take the system out of the validity of the MWT. Notable examples include tethered membranes [2], where one finds a finite- $T$  crumpling transition and a low- $T$  statistically flat phase with long-range orientational order [2] at 2D. Symmetric inhomogeneous fluid membranes form a closely related example; see Ref. [3]. Here a phase transition is obtained between a phase with a finite persistence length and a phase with a diverging persistence length (or equivalently, a *stiffening transition*), tuned by the coupling constant that couples the local curvature with the local inhomogeneity order parameter. However, true LRO does not exist even in the phase with diverging persistence length in Ref. [3]. The latter phase is found to be characterized by a diverging bending modulus in the long-wavelength limit at 2D.

The classical  $O(N)$  nonlinear  $\sigma$  model [4] (hereafter NLS) has found wide usage in a variety of topics, including condensed matter systems [5], mathematical physics [6], particle

physics [7], and cosmology [8]. This is a paradigmatic model with continuous symmetries [4,9], in which the consequence of the MWT is succinctly visible in a low- $T$  expansion. At  $d = 2$  in equilibrium, one finds [9] that the model has no finite- $T$  ordered state with LRO. In this article, we ask the following: What can introduce phase transitions and order in NLS at 2D? Taking a cue from the examples of tethered membranes, we expect that the predictions of MWT may be bypassed in the presence of long-range interactions between the  $O(N)$  spins. Since pure NLS has only short-range interactions between the spins, additional degrees of freedom which may create *effective* long-range interactions are required to invalidate the prediction of the MWT here. These additional fields can be interpreted as representing spatiotemporally nontrivial environments coupled to NLS. The model parameters defining pure NLS now get modified or *renormalized* by the coupled additional degrees of freedom. Clearly, any putative LRO in a 2D generalized NLS should depend upon the specific nature of the additional degrees of freedom and their couplings to the  $O(N)$  spins; i.e., the results should be model dependent. Since we are interested in a question of general principle, it is useful to study simple reduced models, where explicit calculations may be done in straightforward ways. To this end, we generalize NLS and construct three different simple variants of NLS by coupling it to additional fields through generic local interactions, one in equilibrium and the others out of equilibrium: We consider a system of NLS that is (i) thermodynamically coupled with Ising spins (hereafter Model I), (ii) dynamically coupled with a Stokesian velocity field that is affected by the feedback from the  $O(N)$  spins (hereafter Model II), and (iii) dynamically coupled with multiplicative noises through symmetry-allowed minimal coupling (hereafter Model III). For Model I and Model II we consider only nonconserved dynamics, while for Model III we consider both nonconserved and conserved dynamics of NLS. In a *low-noise variance* expansion that generalizes the low- $T$  expansion for

\*tirthankar.banerjee@saha.ac.in

†niladri.sarkar@saha.ac.in; niladri2002in@gmail.com

‡abhik.basu@saha.ac.in; abhik.123@gmail.com

the equilibrium NLS, we illustrate the possibility of order in the NLS with additional fields at 2D. Our principal results are as follows. (i) Both Model I and Model II and nonconserved Model III without any long-range noise have the lower critical dimension  $d_L = 2$ ; for  $d > d_L$  all these have a critical point separating a “high-noise” paramagnetic phase with short-range order (SRO) and a “low-noise” ferromagnetic phase with LRO. (ii) In 2D, both Model I and Model II and the nonconserved version of Model III (without any long-range noise) with appropriate choices of the model parameters show phase transitions, tuned by the coupling constants, from a *disordered soft* phase with SRO, where the effective spin stiffness of the  $O(N)$  spins vanishes over a finite system size to a *stiff phase*, where it stiffens significantly, diverging as  $\ln L$  for a system of linear size  $L$ . As a result, in TL the variance of the fluctuations of the transverse components of the spins depend on  $L$  as  $\ln \ln L$  at 2D, a dependence weaker than the standard  $\ln L$  dependence of the variance of the elastic degree of freedom in an elastic Hamiltonian that displays quasi-long-range order (QLRO) in 2D. For  $N = 2$  at 2D this implies a spatial decay of the equal-time spin correlations in powers of the logarithm of the spatial separation with model-dependent exponents. The model dependence of these exponents are reminiscent of the model-dependent exponents that characterizes the well-known algebraic decay in QLRO; nevertheless, the spatial decay here is markedly slower than the algebraic decay in QLRO. In contrast, the conserved version of Model III without any long-range multiplicative noise admits no stiff phase at 2D. (iii) Nonconserved Model III with long-range multiplicative noises can display true LRO at 2D, controlled by the noise amplitude and the relevant coupling constant. However, the conserved version of Model III with long-range multiplicative noises does not display any LRO in 2D. In addition, we also calculate the dynamic exponent  $z$  that characterizes the correlators of the transverse spin fluctuations in the stiff phases at 2D and at the unstable fixed point (FP) separating the paramagnetic and ferromagnetic phases for  $d > 2$ . The remainder of this article is organized as follows. In Sec. II, we provide a short review of NLS. In Secs. III, IV, and V, we construct and analyze our Models I, II, and III, respectively. In Sec. VI we summarize our results. Some of the technical details are available in Appendixes at the end.

## II. SHORT REVIEW ON NLS

The statistical mechanics of NLS with an  $N$ -component spin  $\Phi = (\phi_1, \dots, \phi_N)$  in the presence of an external magnetic field  $h_i$ ,  $i = 1, \dots, N$  in  $d$ -dimensions is described by the free energy functional  $\mathcal{F}_\sigma$  [9],

$$\mathcal{F}_\sigma = \frac{1}{2} \int d^d x [\kappa (\nabla_\alpha \Phi)^2 - h_i \phi_i], \quad (1)$$

where  $\kappa$  is the spin stiffness; we impose  $\Phi^2 = 1$ . By means of a perturbative low- $T$  expansion, it has been shown [9] that the transition temperature  $T_0$  separating the low- $T$  ferromagnetic phase and the high- $T$  paramagnetic phase is given by

$$\frac{T_0}{\kappa} = \frac{2\pi\epsilon}{N-2} \quad (2)$$

at  $d = 2 + \epsilon$ ,  $\epsilon \geq 0$ . Thus,  $T_0$  vanishes at 2D (i.e.,  $d_L = 2$ ), precluding any finite  $T$  ordered phase with LRO. For  $N = 2$  at 2D,  $T_0$  is indeterminate, suggesting that degrees of freedom not included in NLS, e.g., topological defects and amplitude fluctuations, should destroy the order. Similar analyses have been done on the quantum version of the  $O(N)$  nonlinear  $\sigma$  model; see Ref. [10]. We now ask whether or how these results may be significantly modified in the presence of additional degrees of freedom. We construct Models I, II, and III as above to address this issue. To set up the notations clearly, we denote the spin components of an  $O(N)$  spin by roman indices and the components of a vector or an operator in the real or Fourier space by greek indices in the remaining part of this article.

## III. MODEL I: NLS COUPLED WITH ISING SPINS

We study the equilibrium nonconserved relaxational dynamics of NLS coupled with Ising spins. In the spirit of the Landau-Ginzburg coarse-grained approach, we represent the Ising spins by a scalar field  $\psi(\mathbf{x})$ , where  $\mathbf{x}$  is the coordinate in a  $d$ -dimensional space. We start with the combined free energy functional  $\mathcal{F}_I$  for NLS coupled with the Ising spins: Assuming a minimal symmetry-permitted coupling between the Ising spins and the  $O(N)$  spins, we write

$$\mathcal{F}_I = \int d^d x \left[ \frac{\kappa}{2} (\nabla_\alpha \Phi)^2 - \mathbf{h} \cdot \Phi + \frac{r}{2} \psi^2 + \lambda (\nabla_\alpha \Phi)^2 \psi^2 + \frac{1}{2} (\nabla_\alpha \psi)^2 + \frac{u}{4!} \psi^4 \right], \quad (3)$$

where, as before,  $\Phi = (\phi_1, \dots, \phi_N)$ , is an  $N$ -component vector of unit modulus; i.e.,  $\Phi^2 = 1$ . Here  $r = T - T_c$ ,  $T$  being the temperature and  $T_c$  the mean field critical temperature for the second order Ising magnetic transition, with coupling constant  $u > 0$ . Setting  $\psi = 0$  yields Eq. (1);  $\kappa$  is the spin stiffness. For  $N = 2$ , (3) is related to a Ginzburg-Landau model recently proposed in studies on high-temperature superconductors [11]. In (3) the coupling between  $\phi_i$  and  $\psi$  is controlled by the coupling constant  $\lambda$ . With  $T > T_c$ , for all  $\lambda > 0$ ,  $\mathcal{F}_I$  is minimized by uniform states of the fields—i.e.,  $\phi_i = \text{const.}$  and  $\psi = 0$ —whereas, with large enough  $\lambda < 0$ , such a uniform state becomes thermodynamically unstable. We choose  $\lambda > 0$  here. It is constructed such that Eq. (3) is invariant under rotation of the  $O(N)$  spin  $\phi_i$  in the spin space and inversion of the Ising spins  $\psi \rightarrow -\psi$ . Usual order-disorder transitions and relaxational dynamical critical behavior near critical points in a related model in higher dimensions (e.g., three dimensions) have been studied in Ref. [12], where a variety of temperature driven phase transitions separating the disordered and the ordered phases are discussed. Unlike Ref. [12], we here assume that the  $O(N)$  spins are in the ordered state [and hence put a fixed length constraint on the  $O(N)$  spins] and study the effects of the Ising spins coupled with the  $O(N)$  spins via generic symmetry allowed couplings on the putative ordered state of the  $O(N)$  spins at 2D. Since the Ising spins undergo a usual paramagnetic to ferromagnetic transition at  $T_c$ , we focus on the state of the assumed order of the  $O(N)$  spins at  $T = T_c$ .

We are interested in studying the purely relaxational nonconserved dynamics. The equations of motion for  $\Phi$  and

$\psi$  are respectively given by

$$\frac{\partial \Phi}{\partial t} = -\Gamma \frac{\delta \mathcal{F}_I}{\delta \Phi} + \boldsymbol{\theta} = \Gamma [\kappa \nabla^2 \Phi + 2\lambda \nabla_\beta (\psi^2 \nabla_\beta \Phi) + \mathbf{h}] + \boldsymbol{\theta}, \quad (4)$$

and

$$\begin{aligned} \frac{\partial \psi}{\partial t} &= -\Gamma_2 \frac{\delta \mathcal{F}_I}{\delta \psi} + \eta \\ &= \Gamma_2 \left[ -r\psi - 2\lambda \psi (\nabla_\beta \Phi)^2 + \nabla^2 \psi + \frac{u}{3!} \psi^3 \right] + \eta. \end{aligned} \quad (5)$$

Here  $\Gamma$  and  $\Gamma_2$  are the kinetic coefficients of  $\Phi$  and  $\psi$ , respectively. A quick inspection of Eq (4) reveals that  $\psi$  fluctuations contribute positively to  $\kappa$  through the term with coefficient  $\lambda$ . Whether this can compete with the well-known *thermal softening* of  $\kappa$  that is present even in pure NLS [9] can be determined only after a thorough calculation. This remains a major goal of this work. Stochastic functions  $\boldsymbol{\theta}$  and  $\eta$  are zero-mean Gaussian white noises with variances given by (we set Boltzmann constant  $k_B = 1$ )

$$\langle \theta_i(x,t) \theta_j(0,0) \rangle = 2D\Gamma \delta_{ij} \delta(\mathbf{x}) \delta(t), \quad (6)$$

$$\langle \eta(x,t) \eta(0,0) \rangle = 2\Gamma_2 T \delta(\mathbf{x}) \delta(t). \quad (7)$$

We are considering equilibrium dynamics of the coupled system. Hence, the system obeys the fluctuation-dissipation theorem (FDT) [9,10]. This enforces  $D = T$ . Noting that  $T/\kappa$  is a dimensionless number at 2D, we intend to calculate the effective or *renormalized*  $\kappa$  in a low-temperature expansion ( $D/\kappa \ll 1$ ) up to one-loop order. For simplicity, we treat the fluctuations of  $\psi$  up to the harmonic order; i.e., we set  $u = 0$  [13]. For simplicity, we now set  $\Gamma_2 = 1$ .

It is clear that a uniform state of the  $O(N)$  and Ising spins, where the  $O(N)$  and Ising spins are perfectly aligned among themselves, minimizes  $\mathcal{F}_I$ . Such a state may be parametrized as  $\Phi = (1, 0, \dots, 0)$ . Thermal fluctuations should reduce the component of  $\Phi$  along the direction of order. Now assume an *ordered state* at low  $T$  where the  $O(N)$  spin system is assumed to be ordered in a given direction. A convenient parametrization of  $\Phi$  for such a state is  $\Phi = (\sigma, \boldsymbol{\pi})$ . Thus, with  $\sigma \approx 1$  and  $\pi_i, i = 1, \dots, N-1$  are the small transverse fluctuations; hence,  $\boldsymbol{\pi}$  is an  $N-1$ -component vector. We write  $\sigma = \sqrt{1 - \pi^2} \approx 1 - \frac{\pi^2}{2}$ , where  $\pi^2 = \sum_i \pi_i^2$ . We impose the condition  $\Phi^2 = 1$  on the dynamics via imposing a  $\delta$  function  $\delta_1 = \delta[\sigma^2 + \pi^2 - 1]$  on the generating functional to be constructed (see below) from (4) and (5). Notice that the fixed length constraint  $\Phi^2 = 1$  essentially implies  $\Phi \cdot \partial_t \Phi = 0$ ; i.e., the variation in  $\Phi$  takes place normal to  $\Phi$ , or, in other words, there are  $(N-1)$  independent transverse fluctuating degrees of freedom. The latter are to be associated with  $\pi_i$  defined above with  $\sigma \approx 1$ . Thus, the stochastic force  $\boldsymbol{\theta} = \partial_t \Phi + \Gamma \delta \mathcal{F}_I / \delta \Phi$  in (4) must also be purely transverse. This is ensured by imposing a second  $\delta$  function  $\delta_2 = \delta[\hat{\Phi} \cdot \Phi]$  on the associated generating functional [10,14], where  $\hat{\Phi} = (\hat{\sigma}, \hat{\boldsymbol{\pi}})$  is the dynamic conjugate of  $\Phi$  [15]. Clearly,  $\delta_1$  contributes only when  $\sigma = \sqrt{1 - \pi^2}$ . Further, with  $\hat{\Phi} \cdot \Phi = \hat{\sigma} \sigma + \hat{\boldsymbol{\pi}} \cdot \boldsymbol{\pi}$ ,  $\delta_2$  contributes for  $\hat{\sigma} = -\frac{\hat{\boldsymbol{\pi}} \cdot \boldsymbol{\pi}}{\sigma} = -\frac{\hat{\pi}_i \pi_i}{\sqrt{1 - \pi^2}}$ ; here,  $\hat{\pi}_i$  is the dynamic conjugate of  $\pi_i$ .

After inclusion of the constraints in the form of the  $\delta$  functions  $\delta_1$  and  $\delta_2$ , the generating functional for the system is given by (assume  $\mathbf{h}$  is aligned along  $\sigma$  with a magnitude  $h_1$ )

$$\begin{aligned} \mathcal{Z}_I &= \int \mathcal{D}\sigma \mathcal{D}\hat{\sigma} \mathcal{D}\pi \mathcal{D}\hat{\boldsymbol{\pi}} \mathcal{D}\psi \mathcal{D}\hat{\psi} \exp[S_I] \\ &= \int \mathcal{D}\sigma \mathcal{D}\hat{\sigma} \mathcal{D}\pi \mathcal{D}\hat{\boldsymbol{\pi}} \mathcal{D}\psi \mathcal{D}\hat{\psi} \exp \left[ \int d^d x dt \hat{\sigma} \hat{\sigma} \frac{D}{\Gamma} \right. \\ &\quad + \int d^d x dt \frac{D}{\Gamma} \hat{\boldsymbol{\pi}}_j \hat{\boldsymbol{\pi}}_j \\ &\quad - \int d^d x dt \hat{\sigma} \left\{ \frac{1}{\Gamma} \frac{\partial \sigma}{\partial t} - \kappa \nabla^2 \sigma - 2\lambda \nabla_\beta (\psi^2 \nabla_\beta \sigma) - h_1 \right\} \\ &\quad - \int d^d x dt \hat{\boldsymbol{\pi}}_j \left\{ \frac{1}{\Gamma} \frac{\partial \pi_j}{\partial t} - \kappa \nabla^2 \pi_j - 2\lambda \nabla_\beta (\psi^2 \nabla_\beta \pi_j) \right\} \\ &\quad + \int d^d x dt T \hat{\psi} \hat{\psi} - \int d^d x dt \hat{\psi} \{ \partial_t \psi + r\psi - \nabla^2 \psi \\ &\quad + 2\lambda \psi (\nabla_\beta \sigma)^2 + 2\lambda \psi (\nabla_\beta \pi)^2 \} \\ &\quad \left. \times \delta[\sigma^2 + \pi^2 - 1] \delta[\hat{\sigma} \sigma + \hat{\boldsymbol{\pi}} \cdot \boldsymbol{\pi}] \right]. \end{aligned} \quad (8)$$

The functional integrals over  $\sigma$  and  $\hat{\sigma}$  in  $\mathcal{Z}_I$  above may be evaluated by using the two  $\delta$  functions, which yield two Jacobians. Overall, the total Jacobian  $J$  evaluates to  $(1 - \pi^2)$ , appearing at every  $\mathbf{x}$  and  $t$ . Thus, the contribution of the total Jacobian to  $\mathcal{Z}$  is a product of all these terms, *viz.* [9,15],

$$\begin{aligned} \Pi_{x,t} J &= \Pi_{x,t} (1 - \pi^2) = \exp \left[ - \sum_x \int dt \ln(1 - \pi^2) \right] \\ &= \exp \left[ -\rho \int d^d x dt \ln(1 - \pi^2) \right], \end{aligned} \quad (9)$$

where  $\rho$  is a number equal to the number of degrees of freedom per unit volume that introduced while going from summation to integration. We now expand the nonlinear terms up to  $O(T/\kappa)$ , since we are interested in a low- $T$  one-loop expansion. We obtain the action functional after truncating to the linear order in  $(T/\kappa)$

$$\begin{aligned} S_I &= \int d^d x dt \left[ \frac{D}{\Gamma} \hat{\boldsymbol{\pi}}_j \hat{\boldsymbol{\pi}}_j - \hat{\boldsymbol{\pi}}_j \left\{ \frac{1}{\Gamma} \frac{\partial \pi_j}{\partial t} - \kappa \nabla^2 \pi_j \right. \right. \\ &\quad \left. \left. - 2\lambda \nabla_\beta (\psi^2 \nabla_\beta \pi_j) \right\} + \frac{D}{\Gamma} (\hat{\boldsymbol{\pi}}_j \pi_j)^2 \right. \\ &\quad + \frac{1}{2} \hat{\boldsymbol{\pi}}_j \pi_j \left\{ -\frac{1}{\Gamma} \frac{\partial \pi^2}{\partial t} + \kappa \nabla^2 \pi^2 - 2h_1 (1 + \pi^2/2) \right\} \\ &\quad + T \hat{\psi} \hat{\psi} - \hat{\psi} \{ \partial_t \psi + r\psi \\ &\quad \left. - \nabla^2 \psi + 2\lambda \psi (\nabla_\beta \pi)^2 \} + \rho \pi^2 \right]; \end{aligned} \quad (10)$$

see Appendix A for details. Notice that while the contribution from  $J$  nominally yields a quadratic term of the form  $\rho \pi^2$ , it is  $O(T/\kappa)$  [16]; see also Appendix A. It is convenient to work in the Fourier space; we define  $\mathbf{q}$  and  $\omega$  as the Fourier wave vector and frequency, respectively. At  $T > T_c$ , the fluctuations in  $\psi$  are short lived and small; as a result, the contributions to the measurable physical quantities from the  $\psi$  fluctuations are

small for  $T > T_c$  [17]. In contrast, the  $\psi$  fluctuations diverge in the long-wavelength limit as  $T \rightarrow T_c$ . Similarly,  $\pi_i$  being a broken symmetry mode (i.e., a Goldstone mode), correlation  $\langle |\pi_i(\mathbf{q}, t)|^2 \rangle$  diverges in the long wavelength limit at all  $T$ . Thus, contributions to the measurable quantities from  $\psi$  fluctuations can compete with those originating from the broken symmetry mode fluctuations only near the critical point, i.e., as  $T \rightarrow T_c$ . Hence, in our subsequent analysis below in this section, we set  $D = T = T_c$ . In order to deal with these long-wavelength divergences in a systematic manner, we employ Wilson momentum shell dynamic renormalization group (DRG) [9,18]; see also Ref. [10] for detailed discussions on DRG applications to dynamic critical phenomena. To this end, we first integrate out fields  $\pi_i(\mathbf{q}, \omega), \psi(\mathbf{q}, \omega), \hat{\pi}_i(\mathbf{q}, \omega), \hat{\psi}(\mathbf{q}, \omega)$  with wave vector  $\Lambda/b < q < \Lambda, b > 1$ , perturbatively up to the one-loop order in (10). Here  $\Lambda$  is an upper cut off for wave vector. This allows us to obtain the “new” model parameters corresponding to a modified action  $S_I^<$  with an upper cutoff  $\Lambda/b < \Lambda$ . We obtain

$$\kappa^< = \kappa \left[ 1 + \Delta + 2 \frac{\lambda}{\kappa} \tilde{\Delta} \right], \quad (11)$$

$$\left( \frac{D}{\Gamma} \right)^< = \frac{D}{\Gamma} [1 + \Delta], \quad (12)$$

$$\frac{1}{\Gamma^<} = \frac{1}{\Gamma} [1 + \Delta], \quad (13)$$

$$h_1^< = h_1 \left[ 1 + \frac{N-1}{2} \Delta \right]. \quad (14)$$

Here superscript  $<$  refers to the parameters in the action with a reduced upper cutoff  $\Lambda/b$ . Notice that  $(D/\Gamma)^<$  and  $1/\Gamma^<$  have the same form, which is a consequence of the FDT. Furthermore,

$$\Delta = \int_{\Lambda/b}^{\Lambda} \frac{d^d q}{(2\pi)^d} \frac{D}{(\kappa q^2 + h_1)}, \quad \tilde{\Delta} = \int_{\Lambda/b}^{\Lambda} \frac{d^d q}{(2\pi)^d} \frac{T}{r + q^2}, \quad (15)$$

where we have used the forms of the correlators given in (Appendix B). Clearly, at 2D  $\Delta$  is log divergent for small  $h_1$ , while  $\tilde{\Delta}$  is log divergent at  $r (= T - T_c) = 0$ .

In order to extract the renormalized parameters, we then rescale wave vectors and frequencies according to  $\mathbf{q}' = b\mathbf{q}$  and  $\omega' = b^z \omega$ , where  $z$  is the dynamic exponent. Under these rescalings, fields  $\phi_i, \hat{\phi}_i$  also scale. We write  $\hat{\phi}_i \rightarrow \hat{\xi} \hat{\phi}'_i, \phi_i \rightarrow \xi \phi'_i$  under the above rescalings. FDT in the present model implies that  $\text{Im} \langle \hat{\pi}_i \pi_i \rangle$  and  $\omega \langle \pi_i \pi_i \rangle$  must scale in the same way under the above rescalings (Im refers to the imaginary part). This consideration yields  $\hat{\xi} = \xi b^{-z}$ . With this, rescaling factors for the various model parameters may be obtained. These lead to the renormalized parameters

$$h'_1 = b^{-d-z} \hat{\xi} \xi h_1 \left[ 1 + \frac{(N-1)}{2} \Delta \right], \quad (16)$$

$$\kappa' = \kappa \hat{\xi} \xi b^{-(d+z+2)} \left[ 1 + \Delta + \frac{2\lambda}{\kappa} \tilde{\Delta} \right], \quad (17)$$

$$\left( \frac{D}{\Gamma} \right)' = \hat{\xi}^2 b^{-(d+z)} \frac{D}{\Gamma} [1 + \Delta], \quad (18)$$

$$\left( \frac{1}{\Gamma} \right)' = b^{-(d+2z)} \hat{\xi} \xi \frac{1}{\Gamma} [1 + \Delta]. \quad (19)$$

Notice that with  $\hat{\xi} = \xi b^{-z}$ , the left hand sides of Eqs. (18) and (19) scale in the same way. This is a consequence of the FDT as mentioned above.

In general, the external magnetic field  $\mathbf{h}$  itself is an  $O(N)$  vector that couples with the  $O(N)$  spin  $\Phi$  through the coupling with the external magnetic field given by  $-\int h_j \phi_j d^d x$  in the free energy. Now consider the coupling  $-\int h_j \pi_j d^d x$  in the free energy (3), which would produce a term  $\int h_j \hat{\pi}_j d^d x dt$  in the corresponding action functional (10). Requiring this “external part” of the action to be invariant under rescaling implies  $\int h_j \hat{\pi}_j d^d x dt = \int h'_j \hat{\pi}'_j d^d x' dt'$ . Since the  $O(N)$  symmetry of the problem with  $h_i = 0$  ensures that  $\pi_i$  scales the same way as  $\sigma$ , we have  $h'_i = \hat{\xi} h_i$ ; see Ref. [9] for similar arguments for pure NLS. Due to the  $O(N)$  symmetry of the model for  $h_i = 0$ , all components of  $h_i$  must scale in the same manner. Hence,

$$h'_1 = \hat{\xi} h_1. \quad (20)$$

Using Eqs. (16) and (20), we now evaluate  $\xi$  and  $\hat{\xi}$ :

$$\xi = b^{d+z} \left[ 1 - \frac{(N-1)}{2} \Delta \right], \quad (21)$$

$$\hat{\xi} = b^d \left[ 1 - \frac{(N-1)}{2} \Delta \right]. \quad (22)$$

These yield

$$\kappa' = \kappa b^{d-2} \left[ 1 - (N-2)\Delta + \frac{2\lambda}{\kappa} \tilde{\Delta} \right]. \quad (23)$$

We set  $D = T = T_c$  and are interested in the fluctuation corrections at  $d = 2 + \epsilon, \epsilon > 0$ . At the leading order in  $\epsilon$ , we evaluate  $\Delta$  and  $\tilde{\Delta}$  above at  $d = 2$ . We thus find  $\Delta = \frac{T_c}{2\pi\kappa} \ln b$  for small  $h_1$  and  $\tilde{\Delta} = \frac{T_c}{2\pi} \ln b$ .

We now obtain the continuum flow equations for  $\kappa$  and  $\Gamma$ . Let  $b = e^l, l \rightarrow 0$ , and  $d = 2 + \epsilon$ . Using these definitions and Eq. (23), the differential flow equation for  $\kappa$  becomes

$$\frac{d\kappa}{dl} = \kappa \left[ \epsilon - \frac{(N-2)T_c}{2\pi\kappa} + \frac{2\lambda T_c}{2\pi\kappa} \right]. \quad (24)$$

First consider  $N > 2$ . For  $N - 2 > 2\lambda$ , there is a DRG FP given by  $d\kappa/dl = 0$ . This yields at the unstable FP

$$\frac{T_c}{\kappa} = \frac{2\pi\epsilon}{(N-2) - 2\lambda}, \quad (25)$$

at  $d = 2 + \epsilon$ . Compare (25) with the corresponding result for pure NLS for the (reduced) transition temperature given by (2). Thus, (25) implies a (reduced) transition temperature  $\tilde{T} = T_c/\kappa$  having a value  $\tilde{T}^* \sim O(\epsilon)$  at the FP that separates a low-temperature ferromagnetic phase (ordered state), where the majority of spins are aligned, and a high-temperature paramagnetic phase without any alignment of spins at  $d = 2 + \epsilon$ . Since  $\tilde{T}^* = 0$  at 2D ( $\epsilon = 0$ ), we have  $d_L = 2$ . This physical picture holds for  $N > 2 + 2\lambda$  for which  $T^*$  drops to zero at 2D. At  $N = 2 + 2\lambda$ ,  $T^*$  is indeterminate at 2D. This is the analog of the behavior of the transition temperature for pure NLS with  $N = 2$ . It is understood that topological defects, e.g., vortices and amplitude fluctuations, destroy the order for  $N = 2, d = 2$  in pure NLS [9]. Since  $N$  must be an integer,  $N$  may be increased in steps of unity, where as  $\lambda$  is any real number. Thus,  $\lambda = 1/2$  yields  $N = 3$  such that at  $d = 2$   $T^*$  is



indeterminate for Model I with  $N = 3$ . It will be interesting to study what role, if any, topological defects play to destroy the order there.

In the above analysis, we have assumed the existence of an unstable FP, which may be ensured by choosing  $\lambda$ , a free parameter in the model, appropriately. For  $N < 2 + 2\lambda$ ,  $d\kappa/dl > 0$ , thus precluding any FP. To proceed further, we define a critical  $\lambda_c(\epsilon)$ , at which  $\frac{d\kappa}{dl}$  vanishes, as a function of the  $\epsilon$  parameter given by

$$\lambda_c(\epsilon) = \frac{(N-2)}{2} - \frac{\pi\kappa\epsilon}{T_c}. \quad (26)$$

Defining  $\Delta\lambda(\epsilon) = \lambda - \lambda_c(\epsilon)$ , (24) at  $d = 2$  may be written as

$$\frac{d\kappa}{dl} = \frac{T_c\Delta\lambda(\epsilon=0)}{\pi}, \quad (27)$$

giving an unstable FP  $\lambda = \lambda_c(\epsilon=0) = (N-2)/2$  at 2D. This is reminiscent of a usual equilibrium second order phase transition; nonetheless, there are significant differences that we elaborate below.

Consider now the scale-dependent or renormalized  $\kappa(l)$  at an off-critical point ( $\lambda \neq \lambda_c$  or  $\Delta\lambda \neq 0$ ). Clearly from Eq. (27), for  $\Delta\lambda(\epsilon=0) < 0$ ,  $\kappa(l)$  reduces linearly with  $l$  at 2D and ultimately becomes zero at a particular length scale depending on  $\kappa_0$  and  $\lambda$ . Thus, even for NLS coupled to Ising spins at  $T_c$ , with  $\lambda < \lambda_c(\epsilon=0)$ ,  $\kappa$  vanishes for a sufficiently large system at 2D. The discrete recursion relation for  $\kappa$  at 2D is given by

$$\kappa = \kappa_0 - \frac{(N-2)T_c}{2\pi} \ln b + \frac{\lambda T_c}{\pi} \ln b, \quad (28)$$

where  $\kappa_0$  is a microscopic stiffness. Further writing  $\ln b = \ln(\Lambda/q) = -\ln(qa_0)$ , where  $a_0 \sim$  a microscopic length, we obtain the  $q$  dependence of  $\kappa$ :

$$\kappa(q) = \kappa_0 + \frac{(N-2)T_c}{2\pi} \ln(qa_0) - \frac{\lambda T_c}{\pi} \ln(qa_0). \quad (29)$$

Evidently, the second and third terms of (29) reveal the competition between thermal softening of  $\kappa$  and its stiffening due to the  $\psi$  fluctuations. Not surprisingly, the wave-vector-dependent effective or renormalized  $\kappa$  does not depend upon  $\Gamma$ , a kinetic coefficient. This is again a consequence of the FDT-obeying dynamics. Equation (29) allows us to define a persistence length  $\zeta \sim 1/q$ , such that  $\kappa(\zeta) = 0$  (see, e.g., [3,19] for similar persistence lengths in different problems). This yields

$$\zeta = a_0 \exp\left[\frac{2\pi\kappa_0}{(N-2)T_c - 2\lambda T_c}\right]. \quad (30)$$

Hence, as  $\lambda \rightarrow \lambda_c(\epsilon=0) = \frac{(N-2)}{2}$  in 2D, the persistence length  $\zeta \rightarrow \infty$ . Given the physical interpretation that  $\zeta$  is a typical length scale at which  $\kappa(\zeta) = 0$ , the system remains ordered over a length scale smaller than  $\zeta$ . Thus, for system sizes larger than  $\zeta$ , there will only be SRO. We also define persistence length  $\zeta(\text{NLS})$  for pure NLS ( $\lambda = 0$ )

$$\zeta(\text{NLS}) = a_0 \exp\left[\frac{2\pi\kappa_0}{(N-2)T_c}\right]. \quad (31)$$

Clearly, even for  $\lambda < \lambda_c$ ,  $\zeta(\text{NLS}) < \zeta$ . Thus, even in the soft phase, the persistence length is larger than that for pure NLS, implying that  $\lambda$  in general favors order.

In contrast for  $\lambda > \lambda_c(\epsilon=0)$ ,  $\kappa$  grows on successive applications of momentum shell DRG. Thus, at larger scales NLS is supposed to appear *more ordered* than what it is at smaller scales. Clearly, at higher dimensions, as  $\epsilon$  increases,  $\lambda_c(\epsilon)$  decreases. Hence, at higher dimensions, weaker  $O(N)$ -Ising couplings are enough for  $\kappa(l)$  to grow. Consider now the explicit form for  $\kappa(q)$  in the limit  $q \rightarrow 0$  for  $\lambda > \lambda_c(\epsilon=0)$  at 2D. For  $\lambda - \lambda_c(\epsilon=0) = \Delta\lambda(\epsilon=0) > 0$  at 2D, we have

$$\kappa(q) = -\frac{T_c\Delta\lambda(\epsilon=0)}{\pi} \ln(qa_0) + \kappa_0, \quad (32)$$

which diverges logarithmically in TL ( $q \rightarrow 0$ ). In order to comment on the nature of order, if any, displayed by Model I, we look at the variance of the transverse spin fluctuations  $\pi$ , given by  $\Delta_0 = \langle |\pi_i(\mathbf{q}, t)|^2 \rangle$ , now defined in terms of the renormalized bending modulus  $\kappa(q)$ . We find

$$\begin{aligned} \Delta_0 &= \int \frac{d^2q}{(2\pi)^2} \frac{T_c}{\kappa(q)q^2 + h_1} = -\frac{1}{2\Delta\lambda(\epsilon=0)} \int \frac{dq}{q \ln(qa_0)} \\ &= \frac{1}{2\Delta\lambda(\epsilon=0)} \ln|\ln(a_0/L)| = \frac{1}{2\Delta\lambda(\epsilon=0)} \ln \ln L, \end{aligned} \quad (33)$$

in the limit of large systems, i.e.,  $L \gg a_0$ , where  $L$  is a lower momentum cutoff of the order of the inverse linear system size. Regardless of the value of  $T_c$ , (33) holds as long as  $\lambda > \lambda_c(\epsilon=0)$ . Thus, similar to Ref. [3],  $\Delta_0$  diverges as  $L \rightarrow \infty$ , but very slowly and remains finite for any finite value of  $L$ . In contrast, for pure NLS,  $\kappa(q)$  vanishes for a low enough  $q$ . Hence, for the pure system,  $\Delta_0$  will diverge even for a finite system size. For  $d > 2$ , it may be shown straightforwardly that  $\Delta_0$  is finite in TL. Thus, true LRO exists for  $d > 2$ . A phase diagram of the system in the  $\lambda$ - $\epsilon$  plane is shown in Fig. 1, with the line of FPs given by  $\lambda = \lambda_c(\epsilon)$ , SRO for  $\lambda < \lambda_c(\epsilon)$ , LRO for  $\lambda > \lambda_c(\epsilon)$ ,  $\epsilon > 0$ , and stiff phase for  $\lambda > \lambda_c(\epsilon=0)$ .

It is insightful to consider the flow of the *reduced temperature*  $\tilde{T} = T_c/\kappa$  at 2D. We find

$$\frac{d\tilde{T}}{dl} = \tilde{T}^2 \left[ \frac{N-2}{2\pi} - \frac{2\lambda}{2\pi} \right]. \quad (34)$$

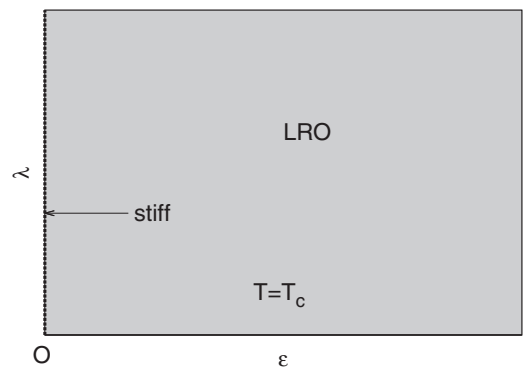


FIG. 1. Phase diagram in the  $\epsilon$ - $\lambda$  plane for  $N = 2$  ( $\lambda_c = 0$ ). The stiff phase exists along the  $\lambda$  axis (broken line,  $\epsilon = 0, \lambda > 0$ ). The symbol  $\circ$  marks the origin  $(0,0)$  and corresponds to pure NLS with SRO at 2D.

For  $\lambda = 0$  and  $N > 2$ ,  $\tilde{T} = 0$  is the only DRG FP. This is, however, an unstable FP (expected), such that even for an arbitrarily small (microscopic)  $\tilde{T} = \tilde{T}_0$ , scale-dependent  $\tilde{T}(l)$  grows. Integrating (34)

$$-\frac{1}{\tilde{T}} = A_0 l + C, \quad (35)$$

where  $A_0 = \frac{N-2}{2\pi} - \frac{2\lambda}{2\pi}$  and  $C$  is a constant of integration. Assume  $A_0 > 0$ . Set at  $l = 0$ ,  $1/\tilde{T} = 1/\tilde{T}_0 > 0$ , we have

$$-\frac{1}{\tilde{T}} = A_0 l - \frac{1}{\tilde{T}_0}. \quad (36)$$

Thus, as  $l \rightarrow 1/(A_0 \tilde{T}_0) \sim \ln \zeta$  from below,  $\tilde{T} \rightarrow \infty$ . This implies that for any microscopic  $\tilde{T}_0 > 0$ , the large scale properties of the system is identical to that of a system at  $\tilde{T} \rightarrow \infty$ , indicating disordered phase at all  $\tilde{T} > 0$ . Since  $T_c$  for an Ising system at 2D is always larger than zero (there is a finite temperature Ising ferromagnetic phase), our Model I at  $T = T_c$  is always in its disordered phase for  $\lambda = 0$ . This scenario changes for  $A_0 < 0$ , or,  $\lambda > \lambda_c$  at 2D. Flow equation (34), upon integration, now yields

$$\frac{1}{\tilde{T}} = |A_0|l + \frac{1}{\tilde{T}_0}. \quad (37)$$

Evidently, for  $l \rightarrow \infty$ ,  $\tilde{T} \rightarrow 0$ . Therefore, for  $\lambda > \lambda_c(\epsilon = 0)$ , scale-dependent  $\tilde{T}(l)$  flows to zero as  $l \rightarrow \infty$ , whereas for  $\lambda < \lambda_c(\epsilon = 0)$ ,  $\tilde{T}(l)$  flows to infinity as  $l \rightarrow \ln \zeta$ . Thus, for  $\lambda > \lambda_c(\epsilon = 0)$ , the properties of the system at the largest (formally TL) scale are expected to be the same as those of the system at zero temperature. This suggests the existence of order in the system. On the other hand, for  $\lambda < \lambda_c(\epsilon = 0)$ , the behavior of the system at large scale is the same as that at infinite temperature, indicating a paramagnetic phase with SRO only. Thus, as  $\lambda$  rises from 0 to a high value through  $\lambda_c(\epsilon = 0)$ , the system undergoes a phase transition from a disordered (paramagnetic) phase to an ordered phase through a critical point at  $\lambda = \lambda_c(\epsilon = 0)$ . This is reminiscent of the usual temperature driven order-disorder second order transition; however, in the present case,  $T$  is kept fixed at  $T_c$  and  $\lambda$  is the tuning parameter.

We now discuss the nature of the order in the ordered phase and whether it is identical to the magnetic (i.e., ferromagnetic) order in usual magnetic systems. The usual magnetic transition is conveniently described by the magnetic order parameter, which is nonzero in the ferromagnetic phase but zero in the paramagnetic phase. Since we assume order in the “1” direction in the spin space, we take  $m = \langle \sigma \rangle = \langle \sqrt{1 - \pi^2} \rangle \approx 1 - \langle \pi^2 \rangle / 2$  as the order parameter. Clearly, in the disordered phase  $m \approx 0$  for a system with a linear size approaching  $\zeta$ . Interestingly, even in the ordered phase,  $m \approx 0$  in TL, due to the divergences found in  $\Delta_0$  above; see Eq. (33). Thus,  $m$  remains zero on *both* sides of the critical point given by  $\lambda = \lambda_c$  and hence cannot work as an order parameter here [20]. Instead, we take

$$\bar{O} = [\ln(\xi/a_0)]^{-1} = -T_c \Delta \lambda / (\pi \kappa_0), \quad (38)$$

with  $\lambda < \lambda_c$  and  $\bar{O} = 0$  with  $\lambda \geq \lambda_c$  as the order parameter at 2D. This is similar to the order parameter defined in the

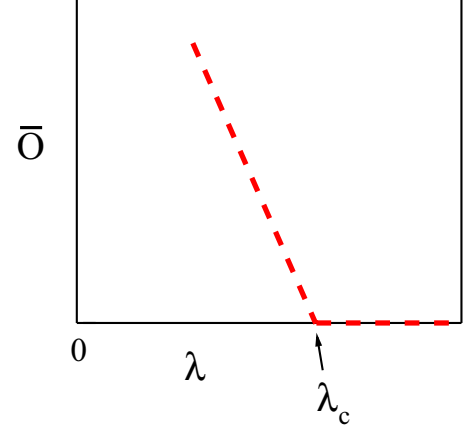


FIG. 2. (Color online) Schematic variation of the order parameter  $\bar{O}$  versus  $\lambda$  in 2D for  $N > 2$ .

context of a crumpled to stiff phase of a heterogeneous fluid membrane [3]. Evidently,  $\bar{O}$  in the soft phase rises smoothly from zero, as  $\lambda$  is reduced from  $\lambda_c$ . Thus, with  $\lambda$  as the control parameter, the *order parameter exponent* is unity. In the stiff phase,  $\bar{O}$  is naturally zero. A schematic plot of  $\bar{O}$  versus  $\lambda$  is shown in Fig. 2. Figures 3 and 4 provide schematic phase diagrams of Model I in the  $N$ - $\lambda$  (with  $T = T_c$ ) and  $\lambda$ - $T$  (for a fixed  $N > 2$ ) planes at 2D [21].

What happens for  $N = 2$  at 2D? In pure NLS, the transition temperature becomes indeterminate, suggesting the importance of topological defects and amplitude fluctuations in destroying LRO in the system. When the O(2) spin is coupled to the Ising spin, the flow equation for  $\kappa(l)$  reduces to

$$\frac{d\kappa}{dl} = \frac{\lambda T_c}{\pi}, \quad (39)$$

giving  $\kappa(q) = \kappa_0 - \lambda T_c \ln(a_0 q) / \pi$  for all  $\lambda > 0$ . Thus, for *any positive*  $\lambda$ , renormalized  $\kappa(l)$  diverges in TL. As a result,  $\Delta_0 \sim [\ln \ln L] / \lambda$  at  $T = T_c$  and the O(2) spins should appear more ordered than the XY model with QLRO at low  $T$ . In an

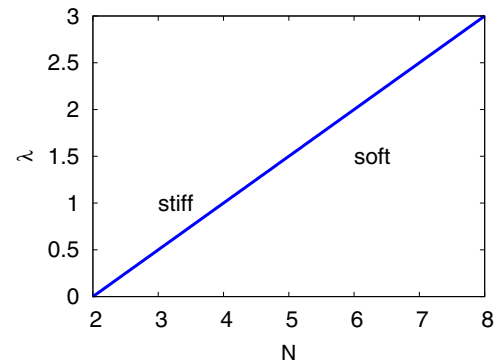


FIG. 3. (Color online) Schematic phase diagram in the  $N$ - $\lambda$  plane at 2D at  $T = T_c$ . The thick line (blue) corresponds to the equation  $\lambda_c(\epsilon = 0) = (N - 2)/2$ . The stiff and soft phases are marked (see text).

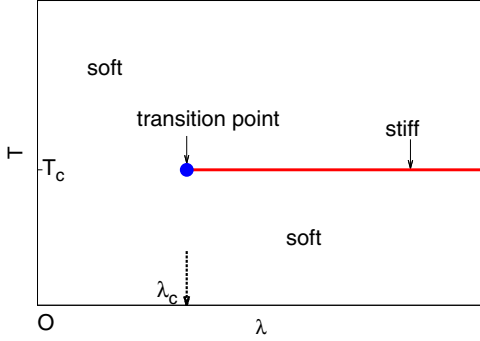


FIG. 4. (Color online) Schematic phase diagram of the  $\lambda$ - $T$  plane for  $N > 2$  at 2D. The symbol  $\circ = (0,0)$  is the origin. Stiff phases exist along the horizontal thick line (red). The solid circle (blue) refers to the critical point  $(\lambda_c, T_c)$ .

equivalent picture, (34) for  $N = 2$  reduces to

$$\frac{d\tilde{T}}{d\lambda} = -\tilde{T}^2 \frac{\lambda}{\pi}. \quad (40)$$

Thus,  $\tilde{T}(\lambda)$  always flows to zero for all  $\lambda > 0$ . Hence, Model I with  $N = 2$  is in its ordered stiff phase for *all*  $\lambda$ . We now calculate the Debye-Waller factor and the equal-time spin-spin correlation  $C_s(r) = \langle \Phi(\mathbf{x}) \cdot \Phi(\mathbf{x}') \rangle$ , for  $N = 2$  in the stiff phase ( $T = T_c, \lambda > \lambda_c$ ), where  $r = |\mathbf{x} - \mathbf{x}'|$  is assumed to be large. For  $N = 2$ , the transverse components  $\pi$  have only one component, say,  $\tilde{\pi}$ ;  $\Phi$  may be expressed as a complex number  $\exp(i\Psi)$ , where  $\Psi(\mathbf{x}, t)$  is a real scalar field; we write  $\Phi_1 = \cos \Psi$ ,  $\Phi_2 = \sin \Psi$  as the two components of  $\Phi$ . For small transverse fluctuations in a nearly ordered state, associate  $\Psi$  with  $\tilde{\pi}$  [equivalently, parametrize  $\Phi = \exp(i\tilde{\pi})$ ; see Appendix D for formulation of the dynamics in terms of  $\Psi$ ]. In the renormalized version of Model I, the variance of  $\tilde{\pi}(\mathbf{x}, t)$  in the stiff phase (for all  $\lambda > 0$ ) in 2D is given by (33), with  $\epsilon = 0$  and  $N = 2$ . Now assuming “1” to be the ordering direction, the average order parameter

$$\begin{aligned} \langle \cos \Psi \rangle &= \exp \left[ -\frac{1}{2} \langle \tilde{\pi}(\mathbf{x}, t)^2 \rangle \right] = \exp \left[ -\frac{1}{2} \Delta_0 \right] \\ &= \exp \left[ -\frac{1}{4\lambda} \ln |\ln L| \right] = \exp(-W) \end{aligned} \quad (41)$$

in (renormalized) Model I for a system of (large) linear size  $L$ . The Debye-Waller factor that determines the depreciation of the magnetization due to the noise induced fluctuations (thermal fluctuations for equilibrium systems) is given by  $\exp(-2W)$ , where  $2W = \Delta_0 = (\ln \ln L)/(2\lambda)$  in the limit of large  $L$  [9]. Clearly,  $W \rightarrow \infty$  in TL here and hence the order parameter vanishes in TL. Note, however, that as  $\lambda$  rises,  $W$  decreases for a fixed  $L$ , and thus, an increase in  $\lambda$  reduces thermal depreciation of the magnetization. Furthermore,

$$\begin{aligned} C_s(r) &= \langle \cos[\Psi(\mathbf{x}, t) - \Psi(0, t)] \rangle \\ &= \text{Re} \langle \exp[i(\Psi(\mathbf{x}, t) - \Psi(0, t))] \rangle = \exp[-g(\mathbf{x})], \end{aligned}$$

where  $g(\mathbf{x}) = \langle [\tilde{\pi}(\mathbf{x}, t) - \tilde{\pi}(0, t)]^2 \rangle / 2 = \int \frac{d^2 q}{(2\pi)^2} [|\tilde{\pi}_{\mathbf{q}}(t)|^2] [1 - \exp(i\mathbf{q} \cdot \mathbf{x})]$ , where we again have made the association between the phase field  $\Phi$  and  $\tilde{\pi}$  for small transverse

fluctuations. Defining  $\mathbf{q} \cdot \mathbf{x} = qr \cos \varphi = u \cos \varphi$ , we obtain in renormalized Model I,

$$\begin{aligned} g(\mathbf{x}) &= -\frac{1}{2\lambda} \int_{rL^{-1}}^{r\Lambda} du \frac{1 - J_0(u)}{u \ln(ua_0/r)} \\ &= -\frac{1}{2\lambda} \int_{rL^{-1}}^1 du \frac{1 - J_0(u)}{u \ln(ua_0/r)} + \frac{1}{2\lambda} \int_1^{r\Lambda} \frac{du J_0(u)}{u \ln(ua_0/r)} \\ &\quad - \frac{1}{2\lambda} \int_1^{r\Lambda} \frac{du}{u \ln(ua_0/r)}, \end{aligned} \quad (42)$$

where  $\Lambda \sim 1/a_0$  is an upper momentum cutoff;  $J_0(u)$  is the zeroth order Bessel function of the first kind. Clearly, the first two terms in the last line of (42) remain finite in TL,  $L \rightarrow \infty$ . Thus, in TL for  $r \rightarrow \infty$  and neglecting the finite parts,

$$g(\mathbf{x}) = \frac{1}{2\lambda} \ln |\ln(a_0/r)|. \quad (43)$$

This gives

$$\begin{aligned} C_s(r) &= \exp \left[ -\frac{1}{2\lambda} \ln |\ln(a_0/r)| \right] \\ &= \frac{1}{|\ln(a_0/r)|^{1/2\lambda}} = \frac{1}{(\ln r)^{1/2\lambda}}, \end{aligned} \quad (44)$$

in the limit  $r \rightarrow \infty$ . Thus, the spatial dependence of  $C_s(r)$  is characterized by a model-dependent exponent  $\lambda$ , which is reminiscent of QLRO in the  $XY$  model below the Kosterlitz-Thouless (KT) transition. Nonetheless, the spatial dependence in (44) is markedly weaker than the algebraic decay of equal-time correlators associated with QLRO [9]. Again for a larger  $\lambda$ ,  $g(\mathbf{x})$  is smaller and the spatial decay of  $C_s(r)$  is accordingly weaker. This is consistent with the role of  $\lambda$  in favoring order in the system.

We now evaluate the dynamic critical exponent  $z$  of the broken symmetry modes  $\pi_i$ . The flow equation for  $\kappa\Gamma$  is obtained as

$$\frac{d}{d\lambda} \kappa\Gamma = \kappa \frac{d\Gamma}{d\lambda} + \Gamma \frac{d\kappa}{d\lambda}. \quad (45)$$

The last term vanishes at  $\lambda \leq \lambda_c(\epsilon)$ , yielding

$$\frac{d}{d\lambda} \kappa\Gamma = -\kappa\Gamma \left[ 2 + \epsilon - z - \frac{(N-2)T_c}{2\pi\kappa} \right]. \quad (46)$$

At the FP, this yields  $z = 2 + \epsilon - \frac{(N-2)T_c}{2\pi\kappa}$ . When  $\lambda \leq \lambda_c(\epsilon)$ ,  $T_c/\kappa = 2\pi\epsilon/[N-2-2\lambda]$  at the DRG FP, which gives  $z = 2 - \frac{2\lambda\epsilon}{(N-2)-2\lambda}$  at the DRG FP. Thus,  $z$  clearly depends on  $\lambda$  and decreases as  $\lambda$  rises for a given  $N$  and  $\epsilon$ . On the other hand, for  $\lambda > \lambda_c(\epsilon)$  and using (24), we find  $z = 2$ , since  $\frac{T_c}{\kappa(L)} \rightarrow 0$  for  $L \rightarrow \infty$  in the stiff phase. Notice that the dynamic exponent  $z_\psi$  for  $\psi$  with a nonconserved relaxational dynamics is  $z_\psi = 2$  to the linear order in  $u$ . In addition, at  $2d$   $z = 2$  at the unstable FP as well. Thus,  $z_\psi = z$  at 2D in general and strong dynamic scaling prevails.

#### IV. MODEL II: NLS COUPLED WITH A STOKESIAN VELOCITY FIELD

Next, we construct a simple nonequilibrium extension of NLS by coupling it to a velocity field  $\mathbf{v}$  dynamically via advection. This may be relevant, e.g., in the dynamics of a

collection of 2D nematic liquid crystals in a 2D flow. These are represented by a unit vector in the coarse-grained limit [22], similar to the  $O(N)$  spins (with  $N = 2$ ). Of course, the dynamics of equilibrium or *active* [23] nematics are far more complex than our simplistic model here; nonetheless, our results in this section may serve as a prototype for the orientational dynamics in systems coupled with an advective velocity field. The usual relaxational equation of motion for  $\Phi$  is then supplemented by an advective nonlinearity. We obtain

$$\partial_t \Phi + \tilde{\lambda} \mathbf{v} \cdot \nabla \Phi = -\Gamma \frac{\delta \mathcal{F}_\sigma}{\delta \Phi} + \boldsymbol{\theta}, \quad (47)$$

where  $\tilde{\lambda}$  is a coupling constant. For simplicity we assume  $\mathbf{v}$  to obey a stochastically forced generalized Stokes equation (neglecting inertia) of the form

$$\eta \nabla^2 v_\alpha - \nabla_\alpha \Pi = \alpha_0 \nabla_\alpha \Phi \cdot \nabla^2 \Phi + f_\alpha. \quad (48)$$

The first term on the right hand side of (48) is a symmetry-allowed feedback of the  $O(N)$  spin on  $\mathbf{v}$ . Such a feedback may originate from a stress tensor due to the  $O(N)$  spins  $\Sigma_{\alpha\beta} = -\alpha_0 \nabla_\alpha \Phi \cdot \nabla_\beta \Phi$ , such that the stress vanishes for  $\Phi = \text{const}$ . This feedback term in (48) is reminiscent of an  $N$ -component generalization of the feedback term in the generalized Navier-Stokes equation for a noncritical binary fluid mixture [24]. We allow the coupling constant  $\alpha_0$  to be both positive or negative. Further,  $\Pi$  is the generalized pressure. Notice that the coupling of  $\Phi$  with  $v_\alpha$  is of *dynamic origin*, unlike in Model I, where such couplings are of static or thermodynamic origin (i.e., can be obtained from a free energy functional). Model II reduces to pure NLS for  $\mathbf{v} = \mathbf{0}$ . Stochastic force  $\mathbf{f}$  is assumed to be zero mean with a Gaussian distribution, having a variance in the Fourier space that is given by

$$\langle f_\alpha(\mathbf{q}, t) f_\beta(-\mathbf{q}, 0) \rangle = D_0 q^2 \delta(t) \delta_{\alpha\beta}. \quad (49)$$

Noise  $\boldsymbol{\theta}$  is again chosen to be a Gaussian zero-mean white noise with a variance given by (6). Note, however, that, being out of equilibrium,  $D$  in (6) no longer has the interpretation of the temperature, although  $D$  still has the same physical dimension as  $T$ . Thus,  $D/\kappa$  continues to be a dimensionless number. In what follows below, we generalize the usual low- $T$  expansion of equilibrium NLS and expand in small  $D/\kappa$ . Apart from the formal similarity between  $D$  here and  $T$ , it is reasonable to expect that a low noise, marked by a low value of  $D$ , should favor setting any order; in contrast, a high value of  $D$  (i.e., high noise) should destabilize it. Thus, an expansion in  $D/\kappa$  is not only a formal generalization of the standard low- $T$  expansion; it is also physically meaningful. We enforce incompressibility on  $\mathbf{v}$ . Thus,  $\Pi$  may be eliminated by imposing  $\nabla \cdot \mathbf{v} = 0$  on (48). We eliminate  $\Pi$  to express  $\mathbf{v}$  as

$$v_\alpha = \frac{\alpha_0 P_{\alpha\beta}}{\eta \nabla^2} (\nabla_\beta \Phi \cdot \nabla^2 \Phi) + \frac{P_{\alpha\beta}}{\eta \nabla^2} f_\beta. \quad (50)$$

Here,  $P_{\alpha\beta} = \delta_{\alpha\beta} - \partial_\alpha \partial_\beta / \nabla^2$  is the transverse projection operator. Equation (50) may be used to eliminate  $\mathbf{v}$  in (47). Evidently,  $v_\alpha$  enters into the dynamics of  $\Phi$  in two distinctly different ways: through (i) the multiplicative noise  $f_\alpha$  and (ii) the deterministic term with the coupling constant  $\alpha_0$ . Now proceeding as for Model I and replacing  $\mathbf{v}$  with (50), we obtain

the action functional

$$\begin{aligned} S_{II} = & \int d^d x dt \left[ \frac{D}{\Gamma} \hat{\pi}_i \hat{\pi}_i - \hat{\pi}_i \left\{ \frac{1}{\Gamma} \frac{\partial \pi_i}{\partial t} - \kappa \nabla^2 \pi_i \right\} + \frac{D}{\Gamma} (\hat{\pi}_i \pi_i)^2 \right. \\ & \left. + \frac{1}{2} \hat{\pi}_i \pi_i \left\{ -\frac{1}{\Gamma} \frac{\partial \pi_j^2}{\partial t} + \kappa \nabla^2 \pi_j^2 - 2h_1 (1 + \pi^2/2) \right\} \right] \\ & - \frac{\tilde{\lambda} \alpha_0}{\Gamma} \int d^d x dt \hat{\pi}_i \left[ \frac{P_{\alpha\beta}}{\eta \nabla^2} (\nabla_\beta \pi_j) (\nabla^2 \pi_j) \right] \nabla_\alpha \pi_i \\ & - \int d^d x dt \lambda \hat{\pi}_i \frac{P_{\alpha\beta}}{\eta \nabla^2} f_\beta \nabla_\alpha \pi_j, \end{aligned} \quad (51)$$

by expanding in (assumed small)  $D/\kappa$ , akin to the Model I above in Sec. III;  $\lambda = \tilde{\lambda}/\Gamma$ ; and  $\pi_i$ ,  $i = 1, \dots, N-1$  is the component of the spin fluctuations transverse to the ordering direction and is a  $(N-1)$ -component vector. Notice that there is no analog of  $T_c$  of Model I in the present study; thus, unlike Model I, we do not restrict ourselves to any particular value of  $D$  (which is the nonequilibrium analog of  $T$  here). As before, in order to proceed systematically, we use Wilson momentum shell DRG to evaluate the loop integrals. Due to the couplings  $\lambda$  and  $\alpha_0$ , there are additional corrections to  $\kappa$  over and above the corrections in the pure NLS model. In particular,  $\kappa$  receives a  $O(\alpha_0 \lambda)$  correction at the lowest order in  $D/\kappa$ . We find

$$\left( \frac{D}{\Gamma} \right)^{<} = \frac{D}{\Gamma} + \frac{D}{\Gamma} \Delta, \quad (52)$$

$$\left( \frac{1}{\Gamma} \right)^{<} = \frac{1}{\Gamma} (1 + \Delta), \quad (53)$$

$$\kappa^{<} = \kappa [1 + \Delta(1 - \mu)], \quad (54)$$

$$h_1^{<} = h_1 + \frac{h_1(N-1)}{2} \Delta, \quad (55)$$

where  $\Delta = \int_{\Lambda/b}^{\Lambda} \frac{d^d q}{(2\pi)^d} \frac{D}{\kappa q^2 + h_1}$ , same as in Model I, and  $\mu = \tilde{\lambda} \alpha_0 / (\kappa \eta \Gamma)$ ; superscript  $<$  has the same implication as in our analysis of Model I above. Since  $\Delta \sim D/\kappa$ , the above one-loop corrections are already  $O(D/\kappa)$ . Thus, we need to find out only  $O(D/\kappa)^0$  corrections, if any, to  $\lambda$  and  $\alpha_0$ . We show in Appendix E that there are, indeed, no corrections to  $\lambda$  and  $\alpha_0$  at  $O(D/\kappa)$ . To evaluate the corrections, we once again employ Wilson momentum DRG. We scale the fields,  $q$ ,  $\Omega$ ,  $\hat{\phi}_i$ , and  $\phi_i$  in the same way as for Model I. The parameters are thus scaled in the following way:

$$h_1' = \hat{\xi} \xi b^{-d-z} h_1 \left[ 1 + \frac{N-1}{2} \Delta \right], \quad (56)$$

$$\left( \frac{D}{\Gamma} \right)' = \hat{\xi}^2 b^{-d-z} \frac{D}{\Gamma} [1 + \Delta], \quad (57)$$

$$\left( \frac{1}{\Gamma} \right)' = \hat{\xi} \xi b^{-(d+2z)} \frac{1}{\Gamma} [1 + \Delta], \quad (58)$$

$$\kappa' = \hat{\xi} \xi b^{-(d+2+z)} \kappa [1 + \Delta(1 - \mu)]. \quad (59)$$

Substituting Eq. (58) in Eq. (57), we obtain

$$D' = \hat{\xi} \xi^{-1} D b^z. \quad (60)$$

In Model I above, we have argued that  $\text{Im} \langle \hat{\pi}_m(\mathbf{q}, \omega) \pi_m(-\mathbf{q}, -\omega) \rangle$  and  $\omega \langle |\pi_m(\mathbf{q}, \omega)|^2 \rangle$  must scale in the same way due to FDT. We used this to set  $D' = D$ .



Model II does not satisfy FDT. Nonetheless, using the freedom to choose one of the rescaling factors ( $\hat{\xi}$  or  $\xi$ ) freely, we continue to impose  $D' = D$ . Thus, from Eq. (60),  $\hat{\xi} = \xi b^{-z}$ . Once again arguing that all components of  $h_i$  should scale in the same manner,  $\xi$  evaluates to  $b^{d+z}[1 - \frac{N-1}{2}\Delta]$ . Hence,  $\hat{\xi} = b^d[1 - \frac{N-1}{2}\Delta]$ .

Using these values of  $\hat{\xi}$  and  $\xi$  in Eq. (59), we get

$$\kappa' = \kappa b^{d-2}[1 - (N-2)\Delta - \mu\Delta]. \quad (61)$$

We substitute  $b = e^l, l \rightarrow 0$  and obtain

$$\frac{d\kappa}{dl} = \kappa \left[ \epsilon - \frac{(N-2)D}{2\pi\kappa} - \frac{\mu D}{2\pi\kappa} \right]. \quad (62)$$

The physical interpretation of (62) follows our analysis of (24) in Model I closely. As long as  $N > 2 - \mu$  there exists a DRG FP for the flow equation (62), such that at the FP we have for the reduced noise strength  $\tilde{D} = D/\kappa$ ,

$$\tilde{D}^* = \frac{2\pi\epsilon}{N-2+\mu}, \quad (63)$$

yielding a (reduced) critical noise strength  $\tilde{D}^* \sim O(\epsilon)$ , demarcating between a ferromagnetic phase (ordered state) at  $\tilde{D} < \tilde{D}^*$  and a paramagnetic phase (disordered state) at  $\tilde{D} > \tilde{D}^*$  at  $d = 2 + \epsilon$ . Equation (63) clearly shows  $d_L = 2$  for Model II. Since the minimum physically realizable value of  $N$  is 2,  $N > 2 - \mu$  for  $\mu > 0$  is always satisfied and, hence, a DRG FP always exists. Thus, for  $N > 2 - \mu$ ,  $\tilde{D}^* = 0$  at 2D, lifting the indeterminacy of the transition for  $N = 2$  NLS at 2D. What this implies about the role of topological defects at 2D for  $N = 2$  requires further investigations. Since, in general,  $\tilde{D}^* = 0$  at 2D for  $\mu > 0$  and  $N \geq 2$ , there is no ordered phase at 2D. This is similar to the results for pure NLS at 2D.

Consider now  $\mu < 0$ . The DRG FP of (62) ceases to exist for  $N < 2 + |\mu|$ . Let us focus at 2D. We define a critical  $\mu_c$  by  $|\mu_c| = N - 2, \mu_c < 0$ , such that at 2D,  $d\kappa/dl = 0$  yields an unstable FP given by  $\mu = \mu_c$  identically [see (62) above]. This again is reminiscent of a second order transition at  $\mu = \mu_c$ ; see discussions for Model I above. Note that for  $N = 2, \mu_c = 0$ . For  $\mu < \mu_c$ , we again obtain a renormalized  $q$ -dependent stiffness  $\kappa(q) = -|\mu|D \ln(a_0q)/(2\pi)$  at 2D, as in Model I above. Naturally, this implies for the variance  $\Delta_0 = (\ln \ln L)/|\mu|$  in 2D for large  $L$ , again similar to Model I. Thus, as  $\mu$  is varied, Model II undergoes a phase transition between a soft phase with a vanishing effective stiffness  $\kappa_e$  for a large enough system and a stiff phase with a diverging  $\kappa_e$  in TL. Nonetheless, this transition for Model II is purely a nonequilibrium transition, due to the nonequilibrium origin of the coupling  $\mu$ . In contrast, the corresponding transition in Model I is an equilibrium phase transition. One can analogously define a persistence length  $\zeta$  such that  $\kappa(\zeta) = 0$ , such that  $\zeta$  remains finite in the disordered phase but diverges as  $\mu \rightarrow \mu_c < 0$  at 2D. As in Model I, the stiff phase for  $\mu < \mu_c$  at 2D has no true LRO; the magnetic order parameter  $m = \langle \sigma \rangle$  vanishes for systems in TL in both the ordered and the disordered phases at 2D and, hence, cannot be used to describe the transition at 2D. Again like Model I, order parameter defined by (38) may be used to delineate the ordered phase from the disordered one. The *order parameter exponent*, unsurprisingly, is 1, the same as in Model I. Notice that for

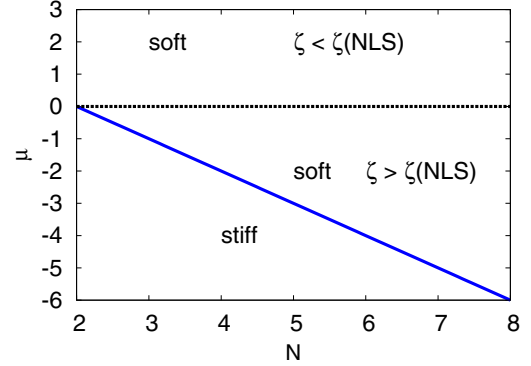


FIG. 5. (Color online) Schematic phase diagram of Model II in the  $N$ - $\mu$  plane at 2D. The solid inclined (blue) line corresponds to the equation  $N = 2 - \mu$ , giving  $\mu_c$ . Soft and stiff phases are marked (see text).

$\mu > 0, \zeta < \zeta(\text{NLS})$ ; hence, an increasing  $\mu$  makes the system more disordered. The flow equation for the scale-dependent reduced noise strength  $\tilde{D}$  may be calculated in analogy with the flow equation for  $\tilde{T}$  in Model I; the associated physical interpretations for the solutions of  $\tilde{D}(l)$  are similar to those for  $\tilde{T}(l)$  in Model I. Specifically, at 2D for  $N = 2$ ,

$$\frac{d\tilde{D}}{dl} = \tilde{D}^2 \frac{\mu}{2\pi}. \quad (64)$$

Thus, for any  $\mu < 0$ ,  $\tilde{D}(l)$  always flows to zero corresponding to the stiff phase, where for any  $\mu > 0$ ,  $\tilde{D}(l)$  diverges as  $l \rightarrow \ln \zeta$ , corresponding to the soft phase. This is consistent with  $\mu_c = 0$  for  $N = 2$ . The Debye-Waller factor  $\exp(-2W)$  and the spin-spin correlation function  $C_s(r)$  for  $N = 2$  at 2D may be calculated in analogy with Model I. Not surprisingly,  $W \rightarrow \infty$  at 2D in the stiff phase ( $\mu < 0$ ), demonstrating the absence of LRO in the stiff phase. In addition,  $C_s(r) \sim [\ln r]^{-1/|\mu|}$  for  $\mu < 0$  and  $r \rightarrow \infty$  at 2D. This is similar to the form of  $C_s(r)$  in Model I stiff phase at 2D, with the model-dependent exponent being determined by  $\mu < 0$ . See Fig. 5 for a schematic phase diagram of Model II in the  $N$ - $\mu$  plane at 2D, highlighting the soft and stiff phases. A corresponding phase diagram of Model II in the  $\epsilon$ - $\mu$  plane is shown in Fig. 6.

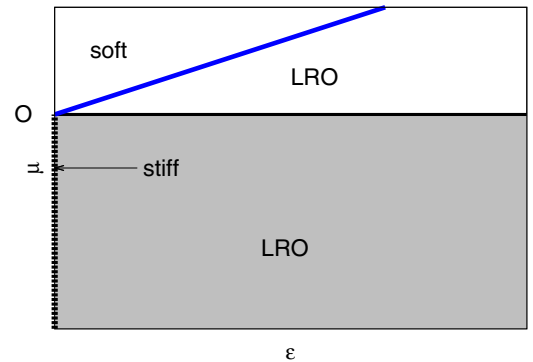


FIG. 6. (Color online) Schematic phase diagram of Model II in the  $\epsilon$ - $\mu$  plane for  $N = 2$ . The symbol  $\circ$  marks the origin,  $(0,0)$ .  $\mu_c = 0$  for  $\epsilon = 0$ . The negative  $\mu$  axis (broken) gives the stiff phase for  $\epsilon = 0$ . The inclined line (blue) corresponds to the equation  $\mu = \frac{2\pi\kappa\epsilon}{D}$  which separates phases with SRO (soft) and LRO for  $\mu, \epsilon > 0$ .

We now evaluate the dynamical critical exponent,  $z$ . Using  $b = e^l, d = 2 + \epsilon$  and Eq. (58), we obtain the flow equation for  $\kappa\Gamma$ ,

$$\frac{d(\Gamma\kappa)}{dl} = \kappa\Gamma \left[ z - 2 - \epsilon + \frac{(N-2)D}{2\pi\kappa} \right] + \kappa\Gamma \left[ \epsilon - \frac{(N-2)D}{2\pi\kappa} - \frac{\mu D}{2\pi\kappa} \right]. \quad (65)$$

At the DRG FP,  $d\kappa/dl = 0$ ; therefore,  $z = 2 + \epsilon - \frac{(N-2)D}{2\pi\kappa}$ , as long as the FP exists. Since for  $\mu > \mu_c$ ,  $D/\kappa = 2\pi\epsilon/(N-2+\mu)$ , we have  $z = 2 + \frac{\mu\epsilon}{N-2+\mu}$  that depends upon  $\mu$  at the DRG FP (similar to the  $\lambda$  dependence of  $z$  at the DRG FP in Model I). On the other hand, for  $\mu < \mu_c$ , we have  $z = 2$  in the stiff phase.

In our above analysis, we have treated  $\mu$  as a *constant* or *number*. This is justifiable provided it can be shown that  $\mu$  is indeed *marginal* under the spatial and temporal rescaling mentioned above. We now show that below. Note that there are no corrections to  $\mu$  at  $O(D/\kappa)^0$ ; see Appendix E. Thus,  $\mu$  is to be affected only trivially under the rescaling of space and time. Consider the term in Eq. (51),  $\lambda \int d^d x dt \hat{\pi}_m \mathbf{v} \cdot \nabla \pi_m$ . In the Fourier space after rescaling of momenta, frequencies, and fields, this term scales as

$$\lambda b^{-2d-2z-1} \hat{\xi} \hat{\xi} \hat{\xi}_v \int d^d q_1 d^d q_2 d\Omega_1 d\Omega_2 \hat{\pi}_m(-\mathbf{q}_1 - \mathbf{q}_2, -\Omega_1 - \Omega_2) \times v_\beta(\mathbf{q}_2, \Omega_2) i q_{1\beta} \pi_m(\mathbf{q}_1, \Omega_1). \quad (66)$$

This yields

$$\lambda' = \lambda b^{-2d-2z-1} \hat{\xi} \hat{\xi} \hat{\xi}_v, \quad (67)$$

where  $\xi_v$  is the corresponding rescaling factor for  $v_\beta(\mathbf{q}, \Omega)$ . Under rescaling  $q' = bq$  and  $\Omega' = b^z \Omega$ , we can write

$$\xi_f^2 \langle f_\alpha(\mathbf{q}'_1, \Omega'_1) f_\beta(\mathbf{q}'_2, \Omega'_2) \rangle = 2D_0 q_1^2 \delta(\mathbf{q}'_1 + \mathbf{q}'_2) \delta(\Omega'_1 + \Omega'_2) b^{d+z-2}, \quad (68)$$

yielding  $\xi_f = b^{(d+z-2)/2}$ , where  $\xi_f$  is the rescaling factor for the noise  $f_\alpha$ . Now apply the same rescaling of wave vectors and frequencies on Eq. (50), yielding in the Fourier space [25]

$$\xi_v v_\alpha(\mathbf{q}', \Omega') = b^{-(d+z+1)} \alpha_0 \xi^2 \left[ \frac{P_{\alpha\beta}}{\eta \nabla^2} (\nabla_\beta \pi_j) \nabla^2 \pi_j \right]_{\mathbf{q}', \Omega'} - \frac{P_{\alpha\beta}(\mathbf{q}')}{\eta q'^2} b^2 \xi_f f_\beta. \quad (69)$$

We choose  $\xi_v = b^2 \xi_f = b^{(d+z+2)/2}$ . We also define  $\alpha'_0 = \alpha_0 \xi_v^{-1} \xi^2 b^{-(d+z+1)}$ . This yields for the scaled coupling constant

$$\mu' = \frac{\lambda' \alpha'_0}{2\eta \kappa' \pi} = \xi^2 b^{-2d-2z} \frac{\lambda \alpha_0}{2\eta \kappa \pi} = \mu, \quad (70)$$

establishing the marginality of  $\mu$  to  $O(D/\kappa)^0$ .

### V. MODEL III: NLS COUPLED WITH MULTIPLICATIVE NOISES

Notice that although Model I and Model II above do display phase transitions for proper choices of the control parameters, the magnetic order parameter remains zero on both sides of the transition point and there is no true LRO in TL at 2D. This sets

them apart from the usual second order magnetic transitions and raises the question what should be a minimal generalized NLS with additional degrees of freedom that may show true LRO in TL at 2D. True LRO in TL requires finite  $\Delta_0$  [see (33) above] in TL at 2D in the stiff phase. In the stiff phases of Model I and Model II,  $\kappa_e(q) \sim -\ln(qa_0)$  in the long-wavelength limit that is responsible for the  $\ln \ln L$  behavior of  $\Delta_0$ . In order to have a finite  $\Delta_0$  in TL,  $\kappa_e(q)$  should diverge more strongly than  $-\ln(qa_0)$  in TL at 2D. It is reasonable to expect that the presence of long-range noises in the system may lead to a finite  $\Delta_0$  in TL at 2D, indicating the existence of true LRO in TL. We study this in this section by using simple reduced models.

In this section, we construct the simplest possible generalizations of NLS by minimally coupling NLS with multiplicative noises of given structures. It remains to be seen how the explicit forms of the couplings with the multiplicative noises affect the long-wavelength properties. Consider first the simple case of a scalar multiplicative noise  $\hat{g}(\mathbf{x}, t)$ , coupled to the  $O(N)$  spin  $\Phi$  via symmetry-allowed minimal couplings. The nonconserved relaxational dynamics of  $\Phi$  is given by

$$\frac{\partial \Phi}{\partial t} + \bar{\lambda} \hat{g} \Phi = -\Gamma \frac{\delta \mathcal{F}_\sigma}{\delta \Phi} + \theta, \quad (71)$$

where  $\bar{\lambda}$  is a coupling constant and  $\hat{g}$  is a zero-mean  $\delta$ -correlated Gaussian white noise with a given variance, say 1;  $\theta$  is a zero-mean Gaussian white noise with a variance given by (6). As before, we use the parametrization  $\Phi = (\sigma, \boldsymbol{\pi})$  and for an assumed nearly ordered state,  $\sigma \approx 1$ . The corresponding generating functional in a compact form is

$$\mathcal{Z}_0 = \int \mathcal{D}\Phi \mathcal{D}\hat{\Phi} \exp \left[ \int d^d x dt \frac{D}{\Gamma} \hat{\Phi} \cdot \hat{\Phi} - \int d^d x dt \hat{\Phi} \cdot \left\{ \frac{1}{\Gamma} \frac{\partial \Phi}{\partial t} + \frac{\bar{\lambda}}{\Gamma} g \Phi + \frac{\delta \mathcal{F}_\sigma}{\delta \Phi} \right\} \right]. \quad (72)$$

Now as before, impose  $\hat{\Phi} \cdot \Phi = 0$ . This evidently eliminates the multiplicative noise term in (72), leaving it identical to that for pure NLS. Thus, the ensuing dynamics is identical to that of pure NLS, with  $\hat{g}$  having no effects on it.

We now generalize  $\hat{g}$  to vector multiplicative noises and study both the nonconserved and conserved dynamics of NLS, coupled to vector multiplicative noises  $a_\alpha$  (with  $d$  components in a  $d$ -dimensional space) via minimal couplings. The corresponding nonconserved and conserved equations of motion of NLS are

$$\frac{\partial \Phi}{\partial t} + \lambda_1 (\mathbf{a} \cdot \nabla) \Phi = -\Gamma \frac{\delta \mathcal{F}_\sigma}{\delta \Phi} + \theta, \quad (73)$$

and

$$\frac{\partial \Phi}{\partial t} + \lambda_2 \nabla \cdot (\mathbf{a} \Phi) = \Gamma \nabla^2 \frac{\delta \mathcal{F}_\sigma}{\delta \Phi} + \nabla_\alpha \Theta_\alpha, \quad (74)$$

respectively. Stochastic noise  $\theta_i$  is Gaussian-distributed with zero mean and variance as given by (6), whereas stochastic noise  $\Theta_{i\alpha}$ , again assumed to be zero-mean Gaussian distributed, has a variance

$$\langle \Theta_{i\alpha}(\mathbf{x}, t) \Theta_{j\beta}(0, 0) \rangle = 2D \Gamma \delta(\mathbf{x}) \delta(t) \delta_{ij} \delta_{\alpha\beta}. \quad (75)$$

In addition,  $a_\alpha$  is a vector (of  $d$  components in a  $d$ -dimensional space) multiplicative noise. We choose  $a_\alpha$  to be

Gaussian-distributed with zero mean and a variance,

$$\langle a_\alpha(\mathbf{q}, t) a_\beta(-\mathbf{q}, 0) \rangle = [m P_{\alpha\beta} + n Q_{\alpha\beta}] \frac{\delta(t)}{q^y}, \quad (76)$$

in the Fourier space. Here  $Q_{\alpha\beta} = q_\alpha q_\beta / q^2 = \delta_{\alpha\beta} - P_{\alpha\beta}$  is the longitudinal projection operator in the Fourier space,  $P_{\alpha\beta}$  is the transverse projection operator defined before. Positivity of  $\langle |a_\alpha(\mathbf{q}, t)|^2 \rangle$  implies  $m(d-1) + n > 0$ , allowing anyone of  $m$  or  $n$  to become negative, subject to the positivity of  $\langle |a_\alpha(\mathbf{q}, t)|^2 \rangle$ . We choose  $y$ , a positive or negative integer, as a free parameter that defines the scaling of (76). The presence of a long-range noise coupled to the  $O(N)$  may be realized in a lattice-gas type model as follows. Imagine a 2D lattice, where sites are occupied by (point) particles, with a spin  $\Phi$  attached to it. Now assume that the particles are nonconserved (due, e.g., to evaporation and absorption); hence, their density fluctuations are short lived and drop out of the dynamical descriptions of the model in the long-wavelength, long-time limit. Now if the particles are subject to Gaussian-distributed random forces (e.g., if the particles are charged and encounter random electromagnetic pulses, but neglect the interparticle interactions) with appropriately chosen variances, effective dynamical equations for the  $O(N)$  spins in this lattice-gas model in the long-wavelength, long-time limit should have the form (73) on symmetry grounds, as the total spin, being attached to the particles, is not conserved. On the other hand, if there are no particle nonconserving events, but the diffusivities of the particles are diverging, then again the density fluctuations relax fast (keeping the spins conserved) and the effective equations of motion for the spin variables should be of the structure as in (74). Notice that we do not specify any particular spin-particle interactions above, as our arguments are sufficiently general and should hold for any short-range interactions between the spins and the particles [26]. While this is a simplistic motivation and Model III is admittedly artificially constructed, it is a reduced model that is purposefully designed to study (i) under what conditions might true LRO set in NLS with additional degrees of freedom in TL at 2D and (ii) whether the nonconserved and conserved dynamics yield the same result in the long-wavelength limit. We see below that our results from Model III are sensitive to the value of  $y$ , such that  $\Delta_0$  may become independent of  $L$  leading to LRO in 2D in the nonconserved version of Model III, but not in its conserved version.

First consider the nonconserved version of Model III. The action functional after expanding up to the linear order in  $D/\kappa$  is (see  $S_I$  and  $S_{II}$ , respectively, for Model I and Model II above)

$$\begin{aligned} S_{III non} = & \int d^d x dt \frac{D}{\Gamma} \hat{\pi}_i \hat{\pi}_i - \int d^d x dt \hat{\pi}_i \left[ \frac{1}{\Gamma} \partial_t \pi_i - \kappa \nabla^2 \pi_i \right] \\ & + \int d^d x dt \frac{D}{\Gamma} (\hat{\pi}_j \pi_j)^2 + \int d^d x dt \frac{1}{2} \hat{\pi}_i \pi_i \\ & \times \left[ -\frac{1}{\Gamma} \frac{\partial}{\partial t} \pi^2 + \kappa \nabla^2 \pi^2 - 2h_1 \left( 1 + \frac{\pi^2}{2} \right) \right] - \frac{\lambda_1}{\Gamma} \\ & \times \int d^d x dt \hat{\pi}_m (\mathbf{a} \cdot \nabla) \pi_m + \rho \int d^d x dt \pi^2. \quad (77) \end{aligned}$$

If  $\lambda_{1s} = \lambda_1 / \Gamma = 0$ , one recovers the usual NLS action. Nonzero  $\lambda_{1s}$  contributes only to  $D/\Gamma$  to the leading order at  $O(\lambda_{1s}^2)$ , viz.,  $\frac{\lambda_{1s}^2}{2} \hat{\pi}_m \hat{\pi}_m \langle (a \cdot \nabla) \pi_n (a \cdot \nabla) \pi_n \rangle$ . This correction evaluates to  $(n\lambda_{1s}^2/2) \int \frac{d^d q}{(2\pi)^d} D/\kappa q^y$ . Hence,

$$\left( \frac{D}{\Gamma} \right)' = \hat{\xi}^2 b^{-(d+z)} \frac{D}{\Gamma} \left[ 1 + \Delta + \frac{n\lambda_{1s}^2 \Gamma}{2D} \bar{\Delta} \right], \quad (78)$$

where,  $\bar{\Delta} = \int \frac{d^d q}{(2\pi)^d} D/(\kappa q^y)$ . Proceeding identically as in Model I and Model II, we obtain for  $D'$ :

$$D' = D b^z \hat{\xi} \xi^{-1} \left[ 1 + \frac{n\lambda_{1s}^2 \Gamma}{2D} \bar{\Delta} \right]. \quad (79)$$

On imposing  $D' = D$ ,

$$\hat{\xi} = \xi b^{-z} \left[ 1 - \frac{n\lambda_{1s}^2 \Gamma}{2D} \bar{\Delta} \right]. \quad (80)$$

Now,  $\kappa' = \kappa \hat{\xi} \xi b^{-(d+z+2)} (1 + \Delta)$ . On substituting  $\xi = b^{d+z} [1 - \frac{N-1}{2} \Delta]$ ,

$$\kappa' = \kappa b^{d-2} \left[ 1 - (N-2)\Delta - \frac{n\lambda_{1s}^2 \Gamma}{2D} \bar{\Delta} \right]. \quad (81)$$

Notice that there is a contribution to  $D'$  with coefficient  $n$  that originates from the multiplicative noise. Its evaluation is given in detail in Appendix F.

We now have three distinct possibilities, namely  $y > 2$ ,  $y < 2$ , and  $y = 2$ . Clearly, for  $y > 2$ , for small  $q$ ,  $\bar{\Delta}$  dominates over  $\Delta$ , whereas, for  $y < 2$ ,  $\bar{\Delta}$  is subdominant. Both terms are equally relevant (in a scaling sense) for  $y = 2$ . It is important to consider the scaling of the parameter  $\chi = \frac{n\lambda_{1s}^2 \Gamma}{2D}$ , which appears as an effective expansion parameter (see below), for an arbitrary  $y$ . To find that, we look at the scaling of  $\lambda_{1s}$  for  $y \neq 2$ . Similar to Eq. (66), we can write

$$\lambda'_{1s} = \lambda_{1s} b^{-2d-2z-1} \hat{\xi} \xi \xi_a, \quad (82)$$

where  $\xi_a$  is the rescaling factor for the field  $\mathbf{a}$ . Using Eq. (76), we evaluate  $\xi_a$ :

$$\xi_a = b^{y/2} b^{(d+z)/2}. \quad (83)$$

Using values of  $\hat{\xi}$ ,  $\xi$ , and  $\xi_a$ , we obtain

$$\lambda'_{1s} = \lambda_{1s} b^{\frac{d-z+y-2}{2}} \left[ 1 - (N-1)\Delta - \frac{n\lambda^2 \Gamma}{2D} \bar{\Delta} \right]. \quad (84)$$

Thus, up to order  $(D/\kappa)^0$ ,  $\lambda'_{1s} = \lambda_{1s}^2 b^{d-z+y-2}$ . Hence,  $\lambda_{1s}^2 \Gamma' = \lambda_{1s}^2 \Gamma b^{y-2} \Rightarrow \chi' = \chi b^{y-2}$ . Thus, with  $b = e^l$  and small  $l$ ,

$$\frac{d\chi}{dl} = \chi(y-2). \quad (85)$$

Therefore,  $\chi$  is marginal for  $y = 2$ , but grows (decays) indefinitely for  $y > (<) 2$ . Let us first consider the case when  $y = 2$ . Using  $\epsilon = d - 2$ ,

$$\frac{d\kappa}{dl} = \kappa \left[ \epsilon - \frac{(N-2+\chi)D}{2\pi\kappa} \right]. \quad (86)$$

As long as  $N-2+\chi > 0$ , FP for the flow equation for  $\kappa$  yields a critical value  $\tilde{D}^*$  for the reduced noise strength

$\tilde{D} \equiv D/\kappa$ . We get

$$\tilde{D}^* = \frac{2\pi\epsilon}{N-2+\chi}, \quad (87)$$

demarcating a ‘‘high-noise’’ paramagnetic disorder phase and a ‘‘low-noise’’ ferromagnetically ordered phase at  $d = 2 + \epsilon$ . At  $d = 2$  and  $\epsilon = 0$ ,  $\tilde{D}^* = 0$ . This then implies the absence of any ferromagnetically ordered state, except for at  $\tilde{D} = 0$ , an analog of  $T = 0$  for equilibrium systems. This again shows that  $d_L = 2$ .

Notice that negative values are allowed for  $n$ ; hence,  $\chi$  can also be negative. Focusing on 2D and with  $\chi_c = -(N-2)$ , we write

$$\frac{d\kappa}{dl} = \frac{(\chi_c - \chi)D}{2\pi} = -\frac{|\chi_c| + \chi}{2\pi} D \equiv \frac{\Delta\chi D}{2\pi}, \quad (88)$$

where  $\Delta\chi = -(|\chi_c| + \chi)$ , giving

$$\kappa = -\frac{(\Delta\chi)D}{2\pi} \ln(qa_0) + \kappa_0, \quad (89)$$

where  $\kappa_0$  is a microscopic stiffness. For  $\chi < 0$  and  $|\chi| > |\chi_c|$ ,  $\Delta\chi > 0$ . Hence,  $\kappa(q)$  diverges logarithmically in TL,  $q \rightarrow 0$ . Hence, the variance of the transverse spin fluctuations  $\Delta_0 \sim \frac{1}{\Delta\chi} \ln \ln L$ . This is reminiscent of our results in the stiff (ordered) phases of Model I and Model II, with  $\chi$  playing the role of the control parameter. For  $\Delta\chi < 0$ , renormalized  $\kappa$  vanishes for a large enough system size, allowing us to define a persistence length  $\zeta$  in direct analogy with Models I and II above. Similar to Model II, we generally find that  $\zeta(\chi > 0) < \zeta(\text{NLS}) < \zeta(\chi < 0)$ . The phase transition from soft to stiff phase may be described by the same order parameter as for Model I and Model II. The flow of the reduced noise strength  $\tilde{D} = D/\kappa$  may be obtained as in Model I and Model II. We find

$$\frac{d\tilde{D}}{dl} = -\tilde{D}^2 \frac{\Delta\chi}{2\pi}, \quad (90)$$

suggesting that for  $\Delta\chi > 0$ ,  $\tilde{D}$  flows to zero in TL, implying an ordered state, whereas for  $\Delta\chi < 0$ ,  $\tilde{D} \rightarrow \infty$  as  $L \rightarrow \zeta$ , indicating a disordered state. This is similar to our analysis for Model I. Notice that  $\chi_c = 0$  for  $N = 2$ . Then following our analysis for Model I, the Debye-Waller factor  $\exp(-2W)$  and the equal-time spin-spin correlator  $C_s(r)$  for  $N = 2$  at 2D may be calculated in the stiff phase at 2D. Not surprisingly and similar to the stiff phases in Model I and Model II, we find  $\exp(-2W) \rightarrow 0$  for  $L \rightarrow \infty$ , precluding any LRO. Furthermore,  $C_s(r) \sim 1/[\ln r]^{|\chi|}$ ,  $\chi < 0$  in the stiff phase at 2D. Again not surprisingly, the spatial decay of  $C_s(r)$  is the same as in the stiff phases of Model I and Model II and characterized by  $|\chi|$ , a model-dependent quantity. A schematic phase diagram of the nonconserved version of Model III in the  $\chi$ - $D$  plane is shown in Fig. 7 ( $d = 2, N = 2$ ).

What happens when  $y \neq 2$ ? Assume  $y > 2$ ; the  $\chi$  term in (81) clearly dominates. Noting that  $\int_{\Lambda/b}^{\Lambda} d^2q/q^y = l/\Lambda^{y-2}$ ,  $b = e^l \approx 1 + l$ , for  $\chi < 0$ , the recursion relation for  $\kappa$  now reads

$$\frac{d\kappa}{dl} = \kappa \left[ \epsilon + \frac{D|\chi(l)|}{2\pi\Lambda^{y-2}\kappa} \right], \quad (91)$$



FIG. 7. Phase diagram of nonconserved Model III in the  $\chi$ - $D$  plane at 2D for  $N = 2$ ,  $y = 2$ . The symbol  $\circ = (0,0)$  is the origin. Stiff ( $\chi < 0$ , renormalized  $D/\kappa \rightarrow 0$ ) and soft with SRO ( $\chi > 0$ , renormalized  $D/\kappa$  diverges) are marked.

where  $\epsilon = d - 2$ . Note that the pure NLS term has been dropped in (91) since it is less infrared divergent than the term arriving from the noise for  $y > 2$ . Now at 2D setting  $\epsilon = 0$ ,  $d\kappa/dl > 0$ , implying  $d_L < 2$ . Solving Eq. (85) and Eq. (91) together, we obtain

$$\begin{aligned} \kappa(l) &= \frac{|\chi|D}{2\pi(y-2)\Lambda^{y-2}}(e^l)^{y-2} + \kappa_0 \\ \Rightarrow \kappa(q) &= \frac{|\chi|D}{2\pi(y-2)}q^{2-y} + \kappa_0, \end{aligned} \quad (92)$$

where  $\kappa_0$  is a microscopic stiffness. Therefore,  $\kappa(q)$  diverges as a power law in  $q$  as  $q \rightarrow 0$ . It should be noted that for  $\chi > 0$ , the recursion relation for  $\kappa$  has the form

$$\frac{d\kappa}{dl} = \kappa \left[ \epsilon - \frac{D\chi(l)}{2\pi\Lambda^{y-2}\kappa} \right]. \quad (93)$$

Hence the  $q$  dependence of  $\kappa$  for  $\chi > 0$  is given by

$$\kappa(q) = \frac{-\chi D}{2\pi(y-2)}q^{2-y} + \kappa_0. \quad (94)$$

Now for  $\chi < 0$ , renormalized variance,  $\Delta_0$ , is given by

$$\begin{aligned} \Delta_0 &= \int_{L^{-1}}^{\Lambda} \frac{dq}{2\pi} \frac{D}{q\kappa(q)} = \frac{|\chi|D}{2\pi} \int_{L^{-1}}^{\Lambda} \frac{dq}{2\pi} \frac{1}{q^{3-y}} \\ &= \frac{|\chi|D}{2\pi(y-2)} \left[ \frac{1}{q^{2-y}} \right]_{L^{-1}}^{\Lambda}, \end{aligned} \quad (95)$$

which gives a finite value for  $\Delta_0$  in TL,  $L \rightarrow \infty$ , indicating true LRO. Consider the Debye-Waller factor  $\exp(-2W)$ , as defined above, and the spin-spin correlation  $C_s(r)$  at 2D for  $N = 2$  with  $\chi < 0$ . Proceeding in analogy with Model I, we find that  $W(= \frac{\Delta_0}{2})$  is finite in TL. Thus, the order parameter does not vanish in TL, indicating LRO in TL. In the same way,

$$g(\mathbf{x}) = \frac{1}{2} \langle [\tilde{\pi}(\mathbf{x}, t) - \tilde{\pi}(0, t)]^2 \rangle = \Delta_0(L \rightarrow \infty), \quad (96)$$

a finite number in the limit  $r \rightarrow \infty$ . Thus,  $C_s(r \rightarrow \infty)$  is finite, consistent with a finite  $W$ , as obtained above. This firmly establishes LRO (ferromagnetic order) for  $\chi < 0, y > 2$  at 2D. Notice that for any  $y > 2$  and  $\chi < 0$ , the system is always in the ordered phase; there is no phase transition at any  $d$ . This is because renormalized  $D/\kappa \rightarrow 0$  in TL at any  $d$  for  $y > 2, \chi < 0$ . The existence of LRO should not come as a surprise, since nonconserved Model III is driven out of equilibrium by the



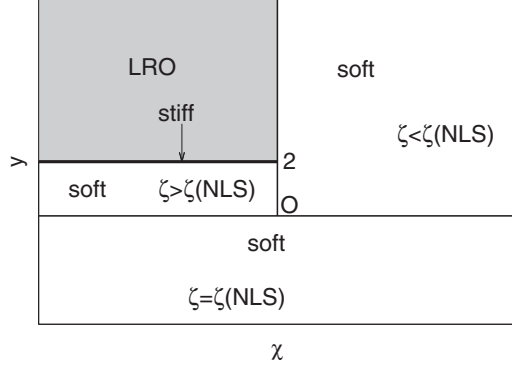


FIG. 8. Phase diagram of nonconserved Model III in the  $\chi$ - $y$  plane at 2D with  $N = 2$ . The symbol  $\circ$  denotes the origin  $(0,0)$ . LRO, soft, and stiff phases are marked.

long-range multiplicative noise. We now briefly consider the consequence of  $\chi > 0$ . Clearly, from (94),  $\kappa(l)$  rapidly drops to zero as the system size approaches the persistence length  $\zeta$  given by

$$\zeta \sim \left[ \frac{\kappa_0(y-2)}{\chi D} \right]^{1/(y-2)}. \quad (97)$$

Thus, nonconserved Model III with  $y > 2$  forms an example of *dynamic second order phase transition* between a disordered state with SRO and an ordered state with LRO with  $\chi$  as a tuning parameter. In dynamic phase transitions, a model goes from one phase to another upon tuning a model parameter of dynamic origin. Well-known examples of dynamic phase transitions include the Kardar-Parisi-Zhang (KPZ) equation for surface growth at dimensions  $d > 2$  [27] and active-to-absorbing state phase transitions [28]. Our nonconserved Model III with  $y > 2$  is an analog of these examples where a continuous symmetry is *dynamically broken*.

Last, for  $y < 2$ , the pure NLS contribution in (81) dominates in the long-wavelength limit, regardless of the sign of  $\chi$ . Thus, in that limit the properties of nonconserved Model III with  $y < 2$  is identical to that of pure NLS, with no order at a finite  $T$  in 2D. A phase diagram of the nonconserved version of Model III in the  $\chi$ - $y$  plane is shown in Fig. 8 with  $d = 2, N = 2$ . In Fig. 9 we provide a phase diagram of nonconserved Model III in the  $y$ - $\epsilon$  plane with  $\chi < 0$ .

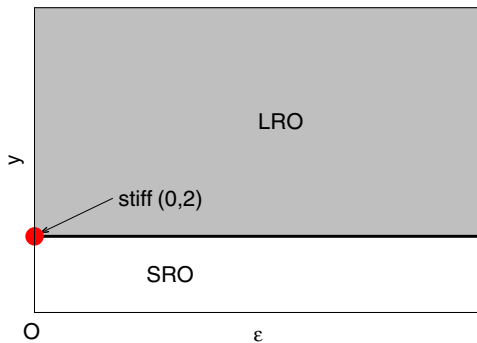


FIG. 9. (Color online) Phase diagram of nonconserved Model III in the  $y$ - $\epsilon$  plane. Regions in the phase space with LRO, SRO (soft phase), and stiff phase (circle) are marked.

We now calculate the dynamic exponent  $z$  at the DRG FP and in the stiff/LRO phases. For  $y < 2$ , results of the pure NLS ensue, precluding any stiff phase at 2D for all  $N \geq 2$ . On the other hand, for  $y > 2$ ,  $\chi < 0$  we have for the recursion relation for  $\Gamma$ ,

$$\Gamma' = \Gamma b^{z-2-\epsilon} [1 - |\chi| \bar{\Delta}]. \quad (98)$$

The recursion relation for  $\Gamma$  for  $y > 2$  thus takes the following form:

$$\Gamma' = \Gamma b^{z-2-\epsilon} \left[ 1 - \frac{|\chi| D (1 - b^{y-2})}{2\pi(2-y)\Lambda^{y-2}\kappa} \right]. \quad (99)$$

As before, the dynamic exponent  $z$  is obtained from the DRG flow equation for  $\kappa\Gamma$ . Considering  $y > 2$ , using (91) and proceeding as for Model I and Model II, we find  $z = 2$  in the LRO phase. Precisely at  $y = 2$ , again proceeding as for Model I and Model II, we have for  $\chi < 0$

$$z = 2 + \epsilon - \frac{(N-2-|\chi|)D}{2\pi\kappa} \quad (100)$$

at the unstable DRG FP for  $|\chi| < |\chi_c|$ . However, for  $|\chi| > |\chi_c|$ ,  $z = 2$  in the stiff phase, as in Model I and Model II.

We now study the conserved version of Model III. The corresponding action,  $S_{III,con}$  is given by

$$\begin{aligned} S_{III,con} = & \int d^d x dt \frac{D}{\Gamma \nabla^4} (\nabla_\alpha \hat{\pi}_i) (\nabla_\alpha \hat{\pi}_i) \\ & - \int d^d x dt \hat{\pi}_i \left[ -\frac{1}{\Gamma \nabla^2} \partial_t \pi_i - \kappa \nabla^2 \pi_i \right] \\ & + \int d^d x dt \frac{D}{\Gamma \nabla^4} [\nabla(\hat{\pi}_j \pi_j)]^2 + \int d^d x dt \frac{1}{2} \hat{\pi}_i \pi_i \\ & \times \left[ \frac{1}{\Gamma \nabla^2} \frac{d}{dt} \pi^2 + \kappa \nabla^2 \pi^2 - 2h_1 \left( 1 + \frac{\pi^2}{2} \right) \right] \\ & - \frac{\lambda_2}{\Gamma} \int d^d x dt \frac{\pi_m}{\nabla^2} (\mathbf{a} \cdot \nabla) \hat{\pi}_m + \rho \int d^d x dt \pi^2. \end{aligned} \quad (101)$$

The leading contributions to  $D/\Gamma$  come from (i)  $\frac{D}{\Gamma \nabla^4} \nabla_\alpha (\hat{\pi}_i \pi_i) \nabla_\alpha (\hat{\pi}_j \pi_j)$  and (ii) a correction second order in  $\lambda_2/\Gamma$ , viz.,  $\frac{\lambda_2^2}{2\Gamma^2} \frac{(\nabla_\alpha \hat{\pi}_i)(\nabla_\beta \hat{\pi}_j)(a_\alpha \pi_i a_\beta \pi_j)}{\nabla^2}$ ; see Appendix C.

For the conserved model, the correlator,  $\langle \pi_i \pi_j \rangle = \int \frac{d^d q}{(2\pi)^d} \frac{d\Omega}{2\pi} \frac{2D\delta_{ij}}{\Gamma q^2 (\frac{\Omega^2}{\Gamma^2} + \kappa^2 q^4)} = \int \frac{d^d q}{(2\pi)^d} \frac{D}{\kappa q^2} \delta_{ij} = \Delta \delta_{ij}$  (for small  $h_1$ ).

Furthermore,  $\langle a_\alpha \pi_i a_\beta \pi_j \rangle$  evaluates to  $\int \frac{d^d q}{(2\pi)^d} \frac{D}{\kappa q^{y+2}} [m(d-1) + n] \frac{\delta_{\alpha\beta} \delta_{ij}}{d} = \hat{\Delta} \frac{\delta_{\alpha\beta} \delta_{ij}}{d}$ . Using these values, we find

$$\left( \frac{D}{\Gamma} \right)^< = \frac{D}{\Gamma} \left[ 1 + \Delta + \frac{\lambda_2^2}{2\Gamma D} \frac{\hat{\Delta}}{d} \right], \quad (102)$$

$$\frac{1}{\Gamma^<} = \frac{1}{\Gamma} [1 + \Delta], \quad (103)$$

$$\kappa^< = \kappa [1 + \Delta], \quad (104)$$

$$h_1^< = h_1 \left[ 1 + \frac{N-1}{2} \Delta \right]. \quad (105)$$

The contribution to  $D^<$  from the multiplicative noise may still be represented diagrammatically as in Appendix F.

However, its explicit expression is clearly different from the corresponding form for the nonconserved Model III. Using the same scaling procedure for  $q$ ,  $\Omega$ ,  $\hat{\pi}$ , and  $\pi$  as above, we can now write  $\xi = b^{d+z}[1 - \frac{N-1}{2}\Delta]$ . These can be used to write the following rescaled corrected values of the parameters:

$$\left(\frac{D}{\Gamma}\right)' = b^{-(d+z-2)}\hat{\xi}^2 \frac{D}{\Gamma} \left[1 + \Delta + \frac{\lambda_2^2}{2\Gamma D} \frac{\hat{\Delta}}{d}\right], \quad (106)$$

$$\frac{1}{\Gamma'} = b^{-(d+2z-2)}\hat{\xi}\xi \frac{1}{\Gamma} [1 + \Delta], \quad (107)$$

$$\kappa' = b^{-(d+z+2)}\hat{\xi}\xi\kappa [1 + \Delta]. \quad (108)$$

Using Eqs. (106) and (107) and imposing  $D' = D$  as before, we obtain

$$\xi = b^z \hat{\xi} \left[1 + P_1 \frac{\hat{\Delta}}{d}\right], \quad (109)$$

where  $P_1 = \frac{\lambda_2^2}{2\Gamma D}$ . Now using the values of  $\hat{\xi}$  and  $\xi$ ,

$$\kappa' = \kappa b^{d-2} \left[1 - (N-2)\Delta - P_1 \frac{\hat{\Delta}}{d}\right]. \quad (110)$$

Using values of  $\hat{\xi}$ ,  $\xi$ , and  $\xi_a$ , we obtain

$$\left(\frac{\lambda_2}{\Gamma}\right)' = \frac{\lambda_2}{\Gamma} b^{\frac{d-z+y+2}{2}} \left[1 - (N-1)\Delta - P_1 \frac{\hat{\Delta}}{d}\right]. \quad (111)$$

Thus, up to order  $(D/\kappa)^0$ ,  $(\frac{\lambda_2}{\Gamma})^2 = \frac{\lambda_2^2}{\Gamma^2} b^{d-z+y+2}$ . Hence,  $(\frac{\lambda_2}{\Gamma})^2 \Gamma' = (\frac{\lambda_2}{\Gamma})^2 \Gamma b^y \Rightarrow P_1' = P_1 b^y$ . Thus, with  $b = e^l$  and small  $l$

$$\frac{dP_1}{dl} = yP_1 \Rightarrow P_1(l) = P_1 \exp[yl]. \quad (112)$$

Therefore,  $P_1$  is marginal for  $y = 0$ , but grows (decays) indefinitely for  $y > (<)2$ .

The second and third terms in the right hand side of (110) compete when  $y = 0$ . For  $y < 0$ , the pure NLS behavior follows while for  $y > 0$ , the nonequilibrium contribution dominates at small  $q$ . For  $d = 2$ ,  $\int_{\Lambda/b}^{\Lambda} \frac{d^2 q}{2\pi q^{y+2}} = \frac{l}{2\pi \Lambda^y}$ , where,  $b = e^l = 1 + l$  and  $\Lambda$  is an upper wave-number cutoff. Similar to the nonconserved case (see above), here we find for  $y > 0$

$$\frac{d\kappa}{dl} = \kappa \left[ \epsilon - P \frac{D}{2\pi \Lambda^y \kappa} \right], \quad (113)$$

where  $\epsilon = d - 2$  and  $P = \frac{[m(d-1)+n]}{d} P_1$ . Hence,  $dP/dl = \frac{[m(d-1)+n]}{d} dP_1/dl = yP$ . At  $d = 2$ ,

$$\frac{d\kappa}{dl} = -\frac{PD}{2\pi \Lambda^y}. \quad (114)$$

Solving the flow equations for  $P$  and  $\kappa$  together,

$$\begin{aligned} \kappa(l) &= -\frac{PD}{2\pi y \Lambda^y} (e^l)^y + \kappa_0 \\ \Rightarrow \kappa(q) &= -\frac{PD}{2\pi y} q^{-y} + \kappa_0. \end{aligned} \quad (115)$$

Thus, as  $q \rightarrow 0$ , renormalized  $\kappa(q)$  runs away rapidly to large negative values, implying the absence of any stiff phase in TL.

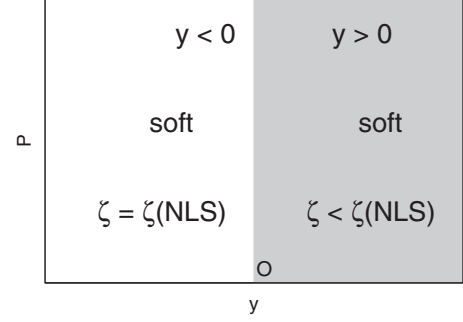


FIG. 10. Phase diagram of nonconserved Model III in the  $y$ - $P$  plane at 2D. Symbol,  $\circ = (0,0)$  denotes the origin. For both positive and negative values of  $y$ , the system remains soft but with different values of  $\zeta$ , as marked in the figure.

The persistence length,  $\zeta$ , at which  $\kappa(q)$  vanishes is given by

$$\zeta \sim \left[ \frac{\kappa_0 y}{PD} \right]^{1/y}, \quad (116)$$

decreasing rapidly as  $y$  increases for fixed  $\kappa_0$ ,  $P$ , and  $D$ ; thus,  $\kappa(l)$  rapidly vanishes to 0 at scale  $\sim \zeta$ . Clearly,  $\zeta < \zeta(\text{NLS})$  for a large enough  $\kappa_0$ . For  $y < 0$ , evidently the results of the pure NLS holds. A schematic phase diagram of the conserved version of Model III in the  $y$ - $P$  plane is shown in Fig. 10 below.

The take home message from this section is that merely the presence of long-range noise does not automatically ensure phase transition to LRO in the system. The detailed mechanism of coupling of the noise with the  $O(N)$  and the underlying dynamics (conserved versus nonconserved) as well as the structure of the noise (e.g., scalar versus vector) are also equally important. Significant differences between nonconserved and conserved dynamics of Model III are not unexpected, as for systems out of equilibrium, the static or equal-time properties obtained from conserved and nonconserved dynamics are not necessarily the same; i.e., the equal-time properties depend on the underlying dynamics. This is in contrast to the well-known equivalence of ensembles in equilibrium systems.

## VI. SUMMARY AND OUTLOOK

In this article, we have addressed phase transitions and the nature of order, if any, in certain generalized NLS constructed by us, where the  $O(N)$  spins are minimally coupled to additional degrees of freedom. To this end, we set up the dynamics of the nonconserved NLS with (i) thermodynamically coupled Ising spins (Model I), (ii) a dynamically coupled Stokesian velocity field (Model II), and (iii) a dynamically coupled vector multiplicative noise (Model III). We also study the conserved version of Model III. In Model I, the couplings are of thermodynamic origin, whereas in Models II and III, the couplings with the additional degrees are of dynamical origin. We use a *low-noise variance expansion*, which for Model I is identical to the well-known low- $T$  expansion for the pure NLS, whereas for Model II and Model III, it is a generalization of the standard low- $T$  expansion. Our studies uncover *unusual phase transitions* in the models as the relevant couplings exceed particular threshold or critical values; in Models I and II and in

the nonconserved version of Model III for  $y = 2$ , the transition is between a *soft phase* with SRO, in which the renormalized spin stiffness  $\kappa$  vanishes in the long-wavelength limit and a *stiff, ordered phase*, where  $\kappa$  diverges as  $\ln L$  in 2D. In the latter phase, the variance  $\Delta_0$  of the transverse spin fluctuations scale proportional to  $\ln \ln L$  with a model-dependent proportionality constant at 2D, a dependence of  $L$  that is substantially weaker than the  $\ln L$  dependence of the broken symmetry modes in classical elastic Hamiltonians that exhibit QLRO. This implies a spatial decay of the equal-time spin-spin correlation function in powers of inverse logarithm of the (large) spatial separation, characterized by model-dependent exponents, at 2D for  $N = 2$ . This model dependence of the exponents are reminiscent of the model-dependent exponents that characterize the algebraic decay of the spin-spin equal-time correlator in the equilibrium XY model displaying QLRO; nevertheless, these power laws of inverse logarithm are distinctly slower varying functions of distance than the algebraic decay in QLRO. Notice that this transition is *not temperature driven*, but rather controlled by the coupling constants at fixed  $T$  or at the fixed noise amplitudes. These transitions have no analog in pure NLS. Nonetheless, the magnetic order parameter remains zero even in the stiff phase in TL at 2D. For  $y > 2$ ,  $\Delta_0$  becomes *independent* of  $L$  even at 2D. This implies LRO in the system. The presence of the long-range multiplicative noise makes the model nonequilibrium and takes it out of the validity of MWT. With  $\chi$  as the tuning parameter, our nonconserved Model III with  $y > 2$  displays a dynamic second order phase transition. We emphasize that there is indeed no clash between our results and MWT. Notice, however, the mere presence of long-range noise itself does not necessarily lead to LRO, e.g., a scalar multiplicative noise minimally coupled to the  $O(N)$  spins have no effect and the model is identical to pure NLS. In addition, the conserved version of Model III does not display any LRO for  $y > 0$ . The lesson, therefore, is that the specific microscopic couplings between the noise and the  $O(N)$  spins may lead to LRO. Furthermore, the conserved version of Model III does not display any phase transition at 2D, unlike its nonconserved counterpart, and has long-wavelength properties that are qualitatively similar to pure NLS. This highlights the lack of *equivalence* between the conserved and nonconserved dynamics of Model III, emphasizing the underlying nonequilibrium nature of the dynamics. We also obtained the dynamic exponent  $z$  at the DRG FP and in the stiff phases of Model I, Model II, and nonconserved Model III, and in the LRO phase of nonconserved Model III with long-range noise.

Our models here are admittedly artificially constructed and simple. Nevertheless, they reveal important physical insight for more realistic but complicated models. We note that, in general, the additional degrees of freedom can affect the dynamics of the  $O(N)$  spins in two different ways: (i) through new effective deterministic couplings for the  $O(N)$  spins and (ii) modification of the noises, e.g., generation of effective noises in the  $O(N)$  spin dynamics. These features should be generic in NLS coupled to other fields. Thus, the basic features of our results should hold. While the Ising spins in Model I have independent dynamics, the overall structure of the coupled dynamical equations is constrained by the FDT. Instead, in Model II, the velocity field being assumed to be

Stokesian, has no independent dynamics, or, in Model III, the multiplicative noise is entirely prescribed by its variance. An obvious generalization would be to consider nonequilibrium coupling with additional fields having their own dynamical evolutions, e.g., coupling with a growing surface described by a generalized KPZ equation [27]. In this model, whether one would find true LRO or an analog of the stiff phase cannot be immediately predicted. Last, we have entirely ignored the topological defects. It is known that in 2D, such defects lead to the KT transition in the equilibrium XY model, where the system undergoes a transition from low- $T$  QLRO with bound pairs of defects to high- $T$  SRO with free defects [9]. It would be interesting to find how the results of the present study may change if the defects are accounted for in the models used here. We look forward to detailed theoretical studies in this direction.

### ACKNOWLEDGMENTS

One of the authors (A.B.) gratefully acknowledges partial financial support by the Max-Planck-Gesellschaft (Germany) and Indo-German Science & Technology Centre (India) through the Partner Group programme (2009).

### APPENDIX A: ACTION FOR MODEL I

We begin with the action functional  $S_I$  for Model I. We perform the following rescalings: (i) Rescale  $t \rightarrow t/\kappa$ , (ii) absorb a factor  $\sqrt{D/\kappa}$  in  $\hat{\pi}_m$ , (iii) absorb a factor of  $\sqrt{\kappa/D}$  in  $\pi_m$ , (iv)  $\psi \rightarrow \sqrt{D}\psi$ , (v)  $\hat{\psi} \rightarrow \hat{\psi}\kappa/\sqrt{D}$ . This ensures that the equal-time correlators  $\langle \pi_m(\mathbf{q}, t)\pi_m(-\mathbf{q}, t) \rangle$  and  $\langle \psi(\mathbf{q}, t)\psi(-\mathbf{q}, t) \rangle$  are independent of the model parameters, and, hence,  $O(D/\kappa)^0$ . We find for the rescaled action

$$S_I = \int d^d x dt \left[ \frac{1}{\Gamma} \hat{\pi}_m \hat{\pi}_m - \hat{\pi}_m \left\{ \frac{1}{\Gamma} \partial_t \pi_m - \nabla^2 \pi_m - \frac{2\lambda D}{\kappa} \nabla_\beta (\psi^2 \nabla_\beta \pi_m) \right\} + \frac{1}{\Gamma} \frac{D}{\kappa} (\hat{\pi}_m \pi_m)^2 + \frac{1}{2} \frac{D}{\kappa} \hat{\pi}_m \pi_m \left( -\frac{1}{\Gamma} \partial_t \pi^2 + \kappa \nabla^2 \pi^2 - \frac{h_1}{\kappa} \pi^2 \right) - \frac{h_1}{\kappa} \hat{\pi}_m \pi_m \right] + \int d^d x dt \frac{1}{\kappa} \rho \pi^2 + \int d^d x dt \times \left[ \hat{\psi} \hat{\psi} \frac{1}{\Gamma_2'} - \hat{\psi} \left( \partial_t \psi \frac{1}{\Gamma_2} + r \psi - \nabla^2 \psi \right) \right], \quad (\text{A1})$$

where  $\Gamma_2' = \frac{D}{T\kappa}$ ,  $\Gamma_2 = 1/\kappa$ . Clearly, *all* the nonlinear terms are  $O(D/\kappa)$ . This justifies our perturbative expansion in small  $D/\kappa$ . Thus, the bare propagator and correlators, which contain only terms that are  $O(T/\kappa)^0$ , after Fourier transforming in space and time are

$$\langle \hat{\pi}_i \pi_j \rangle = \frac{\delta_{ij}}{\frac{-i\omega}{\Gamma} + \kappa q^2 + h_1}, \quad (\text{A2})$$

$$\langle \pi_i \cdot \pi_j \rangle = \frac{2D/\Gamma}{\frac{\omega^2}{\Gamma^2} + (\kappa q^2 + h_1)^2} \delta_{ij}, \quad (\text{A3})$$

$$\langle \hat{\psi} \psi \rangle = \frac{1}{-i\omega + r + q^2}, \quad (\text{A4})$$

$$\langle \psi \psi \rangle = \frac{2T}{\omega^2 + (r + q^2)^2}. \quad (\text{A5})$$

**APPENDIX B: ACTION FOR MODEL II**

Use the same scaling for  $\pi_m$  and  $\hat{\pi}_m$  as in Sec. VI above to obtain

$$\begin{aligned}
S_{II} = & \int d^d x dt \left\{ \frac{1}{\Gamma} \hat{\pi}_m \hat{\pi}_m - \hat{\pi}_m \left[ \frac{1}{\Gamma} \partial_t \pi_m - \nabla^2 \pi_m \right. \right. \\
& \left. \left. - \frac{2\lambda D}{\kappa} \nabla_\beta (\psi^2 \nabla_\beta \pi_m) \right] + \frac{1}{\Gamma} \frac{D}{\kappa} (\hat{\pi}_m \pi_m)^2 + \frac{1}{2} \frac{D}{\kappa} \hat{\pi}_m \pi_m \right. \\
& \left. \times \left[ -\frac{1}{\Gamma} \partial_t \pi^2 + \kappa \nabla^2 \pi^2 - (h_1/\kappa) \pi^2 \right] - (h_1/\kappa) \hat{\pi}_m \pi_m \right\} \\
& + \int d^d x dt \frac{1}{\kappa} \rho \pi^2 - \lambda \alpha_0 \int d^d x dt (D/\kappa) \\
& \times \left[ \hat{\pi}_i \frac{P_{\alpha\beta}}{\eta \nabla^2} (\nabla_\beta \pi_j) (\nabla^2 \pi_j) \nabla_\alpha \pi_i \right]. \quad (\text{B1})
\end{aligned}$$

**APPENDIX C: ACTION FOR MODEL III**

Consider the nonconserved Model III with a vector multiplicative noise  $\mathbf{a}$ . Averaging the generating functional over  $\mathbf{a}$  leads to a term in  $S_{III\text{non}}$  of the form

$$\begin{aligned}
& \lambda_{1s}^2 \int d^d x dt d^d x' dt' \hat{\pi}_m(\mathbf{x}, t) \hat{\pi}_n(\mathbf{x}', t') \\
& \times \langle [\mathbf{a}(\mathbf{x}, t) \cdot \nabla] \pi_m [\mathbf{a}(\mathbf{x}', t') \cdot \nabla] \pi_n(\mathbf{x}', t') \rangle_a, \quad (\text{C1})
\end{aligned}$$

where  $\langle \dots \rangle_a$  implies averaging over the distribution of  $\mathbf{a}$ . Noting that  $\mathbf{a}$  is  $\delta$  correlated in time and then using the same scaling as in Sec. VI above, the new term (C1) above gets a scale factor  $(\lambda_{1s}^2/D)(D/\kappa)$ . Averaging over  $\mathbf{a}$  yields additional factors containing  $m$  and  $n$ ; see (76). This yields a factor  $\sim \chi D/\kappa$  for the contribution to  $D$ . All other terms in  $S_{III\text{non}}$  are the same as those in the action for pure NLS. This establishes the expansion of  $S_{III\text{non}}$  to  $O(D/\kappa)$ . The action  $S_{III\text{con}}$  for conserved Model III may similarly be expanded up to  $O(D/\kappa)$ .

The correlator and propagator terms for conserved Model III are given by

$$\langle \pi_m \pi_n \rangle = \frac{2D/\Gamma}{\frac{\omega^2}{\Gamma^2 q^4} + (\kappa q^2 + h_1)^2} \delta_{mn}, \quad (\text{C2})$$

$$\langle \hat{\pi}_m \pi_n \rangle = \frac{\delta_{mn}}{\frac{-i\omega}{\Gamma q^2} + \kappa q^2 + h_1}. \quad (\text{C3})$$

**APPENDIX D: ALTERNATIVE FORMULATION FOR  $N = 2$** 

In case of  $O(2)$  spins, using  $\Phi^2 = 1$ , we write  $\Phi = \exp[i\Psi]$ . Here phase  $\Psi$  is a Goldstone or broken symmetry mode. Any variation in  $\Phi$  is incorporated as a variation in the phase  $\Psi$ . The equations of motion in terms of  $\Psi$  can thus be written as follows:

Model I,

$$\frac{\partial \Psi}{\partial t} = \Gamma [\kappa \nabla^2 \Psi - 2\lambda \nabla (\psi^2 \nabla \Psi)] + \Theta_\Psi, \quad (\text{D1})$$

Model II,

$$\frac{\partial \Psi}{\partial t} + \lambda \mathbf{v} \cdot \nabla \Psi = \Gamma \kappa \nabla^2 \Psi + \Theta_\Psi; \quad (\text{D2})$$

Model III, nonconserved case,

$$\frac{\partial \Psi}{\partial t} + \lambda_1 \mathbf{a} \cdot \nabla \Psi = \Gamma \kappa \nabla^2 \Psi + \Theta_\Psi; \quad (\text{D3})$$

Model III : Conserved case,

$$\frac{\partial \Psi}{\partial t} + \lambda_2 \nabla \cdot (\mathbf{a} \Psi) = \Gamma \nabla^2 [-\kappa (\nabla^2 \Psi)] + \nabla_\alpha \bar{\Theta}_{\Psi\alpha III}. \quad (\text{D4})$$

Here stochastic noises  $\theta_\Psi$  and  $\Theta_{\Psi_i}$  are zero-mean Gaussian white noises related to the noises  $\theta$  and  $\Theta_i$  above, respectively. In each of the above cases, renormalization of  $\kappa$  may be calculated to the leading order in  $D/\kappa$ , which are identical to the results obtained for Model I, Model II, and Model III above, with  $N = 2$ . Equal-time spin correlation functions  $C_s(r)$  as defined above may be calculated in straightforward ways, yielding the same results as above.

**APPENDIX E: RENORMALIZATION OF  $\kappa$  IN MODEL II**

The term  $\int d^d x dt \lambda \hat{\pi} \frac{P_{\alpha\beta}}{\eta \nabla^2} f_\beta \nabla_\alpha \pi_i$  in the second order evaluates to zero and hence does not contribute to  $\frac{D}{\Gamma}$ .

We now show that there is no renormalization to  $\tilde{\lambda}$  at the one-loop order in Fig. 11.

This evaluates to

$$\begin{aligned}
& \sim \int d^d q d\Omega P_{\alpha\beta}(\mathbf{q}) P_{\alpha\beta}(\mathbf{q}) \frac{\langle f_\gamma(\mathbf{q}, \Omega) f_\delta(-\mathbf{q}, -\Omega) \rangle}{\eta^2 q^4} \\
& \times q_{1\mu} \langle \pi_\mu(-\mathbf{q}, -\Omega) \hat{\pi}_\nu(\mathbf{q}, \Omega) \rangle \langle \pi_\nu(-\mathbf{q}, -\Omega) \hat{\pi}_\gamma(\mathbf{q}, \Omega) \rangle, \quad (\text{E1})
\end{aligned}$$

which vanishes due to causality. Now we show that the coupling constant  $\alpha_0$  has no correction to  $O(D/\kappa)^0$ . The relevant diagram is shown in Fig. 12.

Figure 12 gives a contribution to  $\kappa$ ,

$$\sim \mu \int d^d q_1 d\Omega \hat{\pi}_i P_{\alpha\beta}(\mathbf{q}_1) |\pi_j(\mathbf{q} - \mathbf{q}_1, \omega - \Omega)|^2, \quad (\text{E2})$$

as available in Sec. IV above.

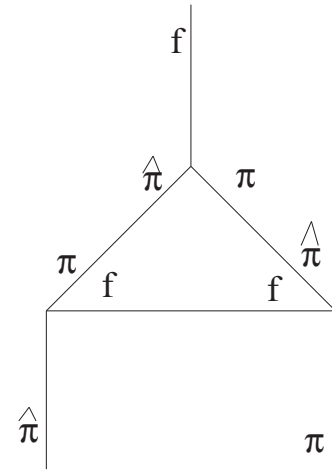
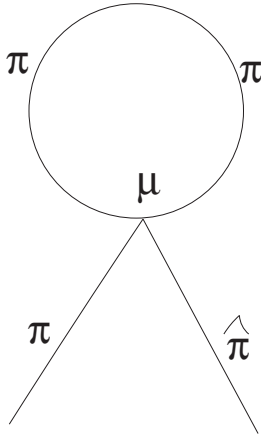


FIG. 11. Feynman diagram for one-loop correction to  $\lambda$  in Model II.



FIG. 12. Feynman diagram for  $O(D/\kappa)$  correction in Model II.

Clearly, the above diagram being proportional to  $\langle \pi_\alpha \pi_\beta \rangle$  is proportional to  $D/\kappa$ . Thus, there are no corrections to  $O(D/\kappa)^0$ .

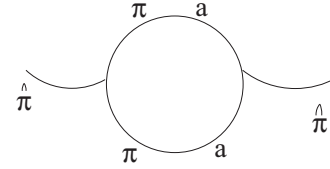


FIG. 13. Feynman diagram for the relevant correction in the nonconserved version of Model III.

#### APPENDIX F: CONTRIBUTION OF THE MULTIPLICATIVE NOISES TO ONE-LOOP CORRECTIONS FOR $D$ IN MODEL III

The one-loop diagram for the contributions up to  $O(D/\kappa)$  to  $\frac{D}{\Gamma}$  in the nonconserved version of Model III is shown in Fig. 13.

- 
- [1] N. D. Mermin and H. Wagner, *Phys. Rev. Lett.* **17**, 1133 (1966); N. D. Mermin, *Phys. Rev.* **176**, 250 (1968).
- [2] D. Nelson, T. Piran, and S. Weinberg (eds.), *Statistical Mechanics of Membranes and Surfaces* (World Scientific, Singapore, 1989).
- [3] T Banerjee and A Basu, *Phys. Rev. E* **91**, 012119 (2015).
- [4] H. E. Stanley, *Phys. Rev. Lett.* **20**, 589 (1968).
- [5] B-G. Liu, *Phys. Rev. B* **45**, 10771 (1992); S. Sachdev and M. Vojta, *ibid.* **68**, 064419 (2003); A. S. Gliozzi and A. Parola, *ibid.* **64**, 184439 (2001); T. Senthil and M. P. A. Fisher, *ibid.* **74**, 064405 (2006); K. Borejsza and N. Dupuis, *ibid.* **69**, 085119 (2004).
- [6] M. Henneaux and A. Wilch, *Phys. Rev. D* **58**, 025017 (1998); A. Alonso-Izquierdo, M. A. G. Leon, and J. M. Guilarte, *Phys. Rev. Lett.* **101**, 131602 (2008); S. Kürkcüoğlu, *Phys. Rev. D* **78**, 065020 (2008).
- [7] H. Falomir and E. M. Santangelo, *Phys. Rev. Lett.* **56**, 1659 (1986); S. R. Das and B. Sathipalan, *ibid.* **57**, 1511 (1986).
- [8] H. Kitamoto and Y. Kitazawa, *Phys. Rev. D* **83**, 104043 (2011); J. Lee, T. H. Lee, T. Y. Moon, and P. Oh, *ibid.* **80**, 065016 (2009).
- [9] P. M. Chaikin and T. C. Lubensky, *Principles of Condensed Matter Physics* (Cambridge University Press, Cambridge, U.K., 2000).
- [10] U. Täuber, *Critical dynamics* (Cambridge University Press, Cambridge, U.K., 2014).
- [11] S. Banerjee, T. V. Ramakrishnan, and C. Dasgupta, *Phys. Rev. B* **83**, 024510 (2011).
- [12] R. Folk, Yu. Holovatch, and G. Moser, *Phys. Rev. E* **78**, 041125 (2008); **79**, 031109 (2009).
- [13] While  $u$  is a *relevant* coupling constant in a renormalization group (RG) sense near  $T_c$  at 2D, at the one-loop order, the only effect of  $u$  is to shift  $T_c$  downward; the dynamic exponent  $z = 2$  and anomalous dimension  $\eta = 0$  at the one-loop order at the critical point, same as their values in the linear theory, i.e., with  $u = 0$  [9, 10]. Hence, treating  $T_c$  as the *one-loop renormalized*  $T_c$ , without any loss of generality, we set  $u = 0$  in what follows below. Effects of a nonzero  $u$  may be included by considering  $\psi$  as the renormalized fields with a nonzero anomalous dimension that becomes nonzero only at  $O(u^2)$ ; the dynamic exponent of  $\psi$  in a relaxational dynamics is also affected at  $O(u^2)$ . Note that the correlation length exponent of  $\psi$  gets corrected at the one-loop order, i.e., at  $O(u)$ . This, however, does not affect out calculations. We have also ignored those contributions to the model parameters defining the dynamics of  $\psi$ , which originates from the fluctuations of the  $O(N)$  spins. These are  $O(T/\kappa)$  in comparison with the fluctuation corrections which originate from the fluctuations of  $\psi$  itself.
- [14] R. Bausch, H. K. Janssen, and Y. Yamazaki, *Z. Phys. B* **37**, 163 (1980).
- [15] C. DeDominicis, *J. Phys. (Paris)* **37**, Colloque C-247 (1976).
- [16] In a dimensional regularization scheme,  $\rho \sim \delta(0) = 0$ ; see, e.g., Ref. [15].
- [17] Fluctuations of  $\psi$  are short lived even for  $T < T_c$ . However, one needs to keep the  $u$  term in (3) for thermodynamic stability. We do not discuss this here in detail.
- [18] P. Hohenberg and B. Halperin, *Rev. Mod. Phys.* **49**, 435 (1977).
- [19] L. Peliti and S. Leibler, *Phys. Rev. Lett.* **54**, 1690 (1985).
- [20] The absence of LRO at 2D even for  $\lambda > \lambda_c(\epsilon = 0)$  is consistent with  $d_L = 2$ .
- [21] While the order parameter  $\bar{O}$  does distinguish the stiff phase from the soft phase, it is unusual as an order parameter in the sense that it is not defined *locally*.
- [22] P. G. de Gennes and J. Prost, *The Physics of Liquid Crystals* (Clarendon Press, Oxford, U.K., 1995).
- [23] M. C. Marchetti, J. F. Joanny, S. Ramaswamy, T. B. Liverpool, J. Prost, and M. Rao, and R. A. Simha, *Rev. Mod. Phys.* **85**, 1143 (2013).
- [24] R. Ruiz and D. R. Nelson, *Phys. Rev. A* **23**, 3224 (1981).
- [25] Note that there is a convolution of the terms  $(\nabla_\alpha \pi_j)(\nabla^2 \pi_j)$  in the Fourier space which yields the scale factor of  $b^{-d-z}$  along with  $b^{-1}$  in Eq. (69).

[26] Note that the *effective* dynamical equations for the  $O(N)$  spins have been written directly, by exploiting the time-scale separations between the fast relaxation of the particle number density fluctuations and the slow relaxation of the broken symmetry  $\pi$  fields. As a result, the particle number densities do not appear as separate dynamical variables in the model equations, but as effective noises with symmetry-permitted structures in the equations for  $O(N)$  spins. The form of these

dynamical equations of the  $O(N)$  spins are, of course, dictated by whether the effective  $O(N)$  spin dynamics is nonconserved or conserved. The former and latter cases may be viewed as *nonequilibrium dynamic analogs* of the grand canonical and canonical ensembles for equilibrium systems, respectively.

[27] M. Kardar, G. Parisi, and Y. C Zhang, [Phys. Rev. Lett. \*\*56\*\*, 889 \(1986\)](#).

[28] H. Hinrichsen, [Adv. Phys. \*\*49\*\*, 815 \(2000\)](#).